

High-Order Staggered Finite Difference Methods for Maxwell's Equations in Dispersive Media

V. A. Bokil* and N. L. Gibson†

Department of Mathematics

Oregon State University

Corvallis, OR 97331-4605

Abstract:

We study the stability properties of, and the phase error present in, several higher order (in space) staggered finite difference schemes for Maxwell's equations coupled with a Debye or Lorentz polarization model. We present a novel expansion of the *symbol* of finite difference approximations, of arbitrary (even) order, of the first order spatial derivative operator. This alternative representation allows the derivation of a concise formula for the numerical dispersion relation for all (even) order schemes applied to each model, including the limiting (infinite order) case. We further derive a closed-form analytical stability condition for these schemes as a function of the order of the method. Using representative numerical values for the physical parameters, we validate the stability criterion while quantifying numerical dissipation. Lastly, we demonstrate the effect that the spatial discretization order, and the corresponding stability constraint, has on the dispersion error.

Keywords: Maxwell's Equations, Debye, Lorentz, higher order FDTD, dissipation, dispersion, phase error.

1 Introduction

The computational simulation of electromagnetic interrogation problems, for the determination of the dielectric properties of complex dispersive materials (such as biological tissue), requires the use of highly efficient forward simulations of the propagation of transient electromagnetic waves in these media. These simulations have very important applications in diverse areas including noninvasive detection of cancerous tumors, and the investigation of the effect of precursors on the human body [11, 1, 2, 18]. Thus, a lot of research has concentrated on the development of accurate, consistent and stable discrete forward solvers.

The electric and magnetic fields inside a material are governed by the macroscopic Maxwell's equations along with constitutive laws that account for the response of the material to the electromagnetic field. Numerical approximation algorithms of time-dependent

*email: bokilv@math.oregonstate.edu

†email: gibsonn@math.oregonstate.edu

wave equations and Maxwell's equations introduce error into the amplitude and speed of the propagating waves. These errors include numerical *dissipation*, the dampening of some frequency modes, and numerical *dispersion*, the frequency dependence of the phase velocity of numerical wave modes in the computational grid. Dielectric materials have actual physical dispersion. The complex electric permittivity of a dielectric medium is frequency dependent (has dielectric dispersion). Thus, an appropriate discretization method should have a numerical dispersion that matches the model dispersion as closely as possible. Dielectric materials also have physical dissipation, or attenuation, which must also be correctly computed by a numerical method.

The Lax-Richtmyer theorem [37] states that the convergence of consistent difference schemes to initial value problems represented by PDE's is equivalent to stability. Hence analysis of stability criteria for conditionally stable schemes is important. The stability and dispersion properties for the finite difference time domain (FDTD) methods, also called Yee schemes, applied to Maxwell's equations in free space are well known (see [40]). There are several FDTD extensions that have been developed to model electromagnetic pulse propagation in dispersive media. One way to model a dispersive medium is to add to Maxwell's equations a set of ordinary differential equations (ODEs) that relate the electric displacement \mathbf{D} to the electric field \mathbf{E} [23], or a set of ODEs that model the dynamic evolution of the macroscopic polarization vector \mathbf{P} driven by the electric field [26, 25]. This technique is known as the auxiliary differential equation (ADE) method. FDTD schemes are constructed for this augmented system by discretizing Maxwell's equations as usual (Yee scheme) and in addition time discretizing the auxiliary ODEs using a second order in time method, so that the fully discretized augmented Maxwell system is second order accurate in space and time. Dielectric dispersion can be expressed in the time domain as a convolution integral involving the electric field and a causal susceptibility function. The recursive convolution (RC) method [28, 29, 27] uses a recursive technique to update the convolution representation of the constitutive law along with the FDTD time update of Maxwell's equations. There are other methods such as the Z-transform [39, 38] and the TLM method [9] that have also been used to model pulse propagation in dispersive media. The discrete versions of many of these modeling approaches have been compared and analyzed for their numerical errors and stability properties [31, 48, 36, 10, 16, 47].

In this paper we consider Maxwell's equations in Debye or Lorentz dispersive media using the ADE approach which results in a system of ODEs appended to Maxwell's equations. The constitutive law in the medium involves a (linear) ODE that describes the dynamic evolution of the polarization driven by the electric field. We consider high order (in space) staggered FDTD like methods for the numerical discretization of the augmented Maxwell system for Debye and Lorentz dispersive media. These methods have $2M$ order accuracy in space and second order accuracy in time. We denote such methods as $(2, 2M)$ order finite difference methods, where $M \in \mathbb{N}$ is arbitrary.

In [32], the author presents an argument in favor of using $(2, 4)$ order finite difference schemes for wave propagation in relaxing dielectrics (Debye media). The author shows that there is a stiff problem in the time direction due to exponential decay in the skin-depth, and with the existence of disparate wave speeds in well defined spatio-temporal regions. In addition, the problem is asymptotically singularly perturbed since it changes type from hyperbolic to parabolic. The $(2, 4)$ schemes, as opposed to the $(2, 2)$ (Yee) scheme, do not

suffer from a phase error degradation as the Courant number is decreased. Due to the time stiffness it is desirable to use a small time step by reducing the Courant number or by increasing the spatial cell size, which can be done with the $(2, 4)$ schemes.

Higher order finite difference methods for the wave equation and for Maxwell's equations in free space have been studied by many authors; see [42, 43, 44, 24, 13, 4] and the references therein. The extensions of higher order staggered finite difference methods to Maxwell's equations in dispersive media have been considered in [46, 45, 34, 33, 35]. In particular [46, 45] developed a $(4,4)$ method for Maxwell's equations in a cold plasma, while [34, 33, 35] considered various 2, 4 and 6th order methods for Debye, Drude and Lorentz media.

Our focus in this paper is the derivation of closed form analytical stability criteria for the staggered $(2, 2M)$ FDTD methods, for arbitrary M . In addition we also derive numerical dispersion relations for these schemes. We obtain information about the expected accuracy of the method from the construction of the numerical dispersion relation which relates the numerical wave number to the frequency for waves propagating in the finite difference grid. We then compare the numerical dispersion relation with the dispersion relation for the corresponding continuous model.

The outline of the paper is as follows. In Section 2 we describe the ADE formulations for Debye and Lorentz type dispersive media in three dimensions, and in Section 3 we consider the one dimensional models. The key result required to perform the stability and dispersion analyzes for arbitrary M is the equivalence of the symbol of the $2M$ order finite difference approximation of the first order derivative operator $\partial/\partial z$ with the truncation of an appropriate series expansion of the symbol of $\partial/\partial z$. This result is proved in Section 4. A similar result has been proved for $2M$ order finite difference approximations of the Laplace operator in [4], which also enabled the authors to derive closed form stability conditions and dispersion relations for $(2, 2M)$ schemes applied to the one-dimensional wave equation.

The $(2, 2M)$ order schemes for Debye and Lorentz media are presented in Section 5. In conjunction with the key result obtained in Section 4, von Neumann analysis is used to obtain stability conditions in Section 6. In [31], the author derived partial stability conditions and numerical dispersion relations for the $(2, 2)$ schemes for Debye and Lorentz dispersive media. These results were valid for certain representative media for each type of dispersive model. In [10], the stability analysis was extended and stability conditions for the $(2, 2)$ schemes for general Debye and Lorentz dispersive media were derived using von Neumann analysis. We use the ideas and results from [10] and [31] and extend the stability analysis to $(2, 2M)$ order staggered finite difference methods. In Section 7 we extend the numerical dispersion analysis in [31] to $(2, 2M)$ schemes. Numerical dispersion relations were not considered in [10]. Stability conditions for the $(2, 4)$ methods for Debye and Lorentz media were derived in [34] using the Routh-Hurwitz criteria and numerical dispersion relations were also considered for the cases $M = 2, 4, 6$. The numerical dispersion analysis was extended to arbitrary (even) order methods in [35], however the representations used led to cumbersome algebra, and the extension to the limiting (infinite order) case is not obvious.

The stability and dispersion analyzes performed in this report are for one dimensional models. However, from these results the extension to two and three dimensions, though tedious, can be easily performed. We present conclusions in Section 8.

2 Model formulation

We consider Maxwell's equations which govern the electric field \mathbf{E} and the magnetic field \mathbf{H} in a domain Ω from time 0 to T given as

$$\frac{\partial \mathbf{D}}{\partial t} + \mathbf{J}_{c,s} - \frac{1}{\mu_0} \nabla \times \mathbf{B} = \mathbf{0} \text{ in } (0, T) \times \Omega, \quad (2.1a)$$

$$\frac{\partial \mathbf{B}}{\partial t} + \nabla \times \mathbf{E} = \mathbf{0} \text{ in } (0, T) \times \Omega, \quad (2.1b)$$

$$\nabla \cdot \mathbf{D} = 0 = \nabla \cdot \mathbf{B} \text{ in } (0, T) \times \Omega, \quad (2.1c)$$

$$\mathbf{E} \times \mathbf{n} = \mathbf{0} \text{ in } (0, T) \times \partial\Omega, \quad (2.1d)$$

$$\mathbf{E}(0, \mathbf{x}) = \mathbf{0} = \mathbf{H}(0, \mathbf{x}) \text{ in } \Omega. \quad (2.1e)$$

The fields \mathbf{D}, \mathbf{B} are the electric and magnetic flux densities respectively. All the fields in (2.1) are functions of position $\mathbf{x} = (x, y, z)$ and time t . We have $\mathbf{J}_{c,s} = \mathbf{J}_c + \mathbf{J}_s$, where \mathbf{J}_c is a conduction current density and \mathbf{J}_s is the source current density. We will assume $\mathbf{J}_c = \mathbf{0}$ in this paper, as we are interested in dielectrics with no free charges. Perfect conducting boundary conditions (2.1d) are added to system to terminate the computational domain.

Constitutive relations which relate the electric and magnetic flux densities \mathbf{D}, \mathbf{B} to the electric and magnetic fields \mathbf{E}, \mathbf{H} are added to these equations to make the system fully determined and to describe the response of a material to the electromagnetic fields. In free space, these constitutive relations are $\mathbf{D} = \epsilon_0 \mathbf{E}$, and $\mathbf{B} = \mu_0 \mathbf{H}$, where ϵ_0 and μ_0 are the permittivity and the permeability of free space, respectively, and are constant [22]. In general there are different possible forms for these constitutive relationships. In a frequency domain formulation of Maxwell's equations, these are usually converted to linear relationships between the dependent and independent quantities with frequency dependent coefficient parameters. We will consider the case of a dispersive dielectric medium in which magnetic effects are negligible. Thus, within the dielectric medium we have constitutive relations that relate the flux densities \mathbf{D}, \mathbf{B} to the electric and magnetic fields, respectively, as

$$\mathbf{D} = \epsilon_0 \mathbf{E} + \mathbf{P}, \quad (2.2a)$$

$$\mathbf{B} = \mu_0 \mathbf{H}. \quad (2.2b)$$

In (2.2a), the quantity \mathbf{P} is called the macroscopic electric polarization. (A discussion of the relationship between the macroscopic polarization and the microscopic material properties leading to distributions of relaxation times and other dielectric parameters in the constitutive laws can be found in [7].) Electric polarization may be defined as the electric field induced disturbance of the charge distribution in a region. This polarization may have an instantaneous component as well as delayed effects; the latter will usually have associated time constants called relaxation times which are denoted by τ . We define the instantaneous component of the polarization to be related to the electric field by means of the free space permittivity, ϵ_0 , and a susceptibility χ . The remainder of the electric polarization, called the relaxation polarization, is denoted as \mathbf{P}_R . Therefore, we have

$$\mathbf{P} = \mathbf{P}_I + \mathbf{P}_R = \epsilon_0 \chi \mathbf{E} + \mathbf{P}_R, \quad (2.3)$$

and hence the constitutive law (2.2a) becomes

$$\mathbf{D} = \epsilon_0 \epsilon_r \mathbf{E} + \mathbf{P}_R, \quad (2.4)$$

where $\epsilon_r = (1 + \chi)$ is the relative permittivity of the dielectric medium. We will henceforth denote \mathbf{P}_R by \mathbf{P} , as the instantaneous polarization will be absorbed into the dielectric constant ϵ_r .

To describe the behavior of the media's macroscopic electric polarization \mathbf{P} ($= \mathbf{P}_R$), we employ a general integral equation model in which the polarization explicitly depends on the past history of the electric field. This model is sufficiently general to include microscopic polarization mechanisms such as dipole or orientational polarization (Debye), as well as ionic and electronic polarization (Lorentz), and other frequency dependent polarization mechanisms [3]. The resulting constitutive law can be given in terms of a polarization or displacement susceptibility kernel g as

$$\mathbf{P}(t, \mathbf{x}) = \int_0^t g(t-s, \mathbf{x}) \mathbf{E}(s, \mathbf{x}) ds, \quad (2.5)$$

For more complex dielectric materials, a simple Debye or Lorentz polarization model is often not adequate to characterize the dispersive behavior of the material. One can then turn to combinations of Debye, Lorentz, or even more general n^{th} order mechanisms [6] as well as Cole-Cole type (fractional order derivative) models [15]. Additionally, materials may be represented by a distribution of the associated time constants or even a distribution of polarization mechanisms (see [8, 7]).

In this paper we concentrate our analysis on single pole Debye and Lorentz polarization models.

2.1 Orientational Polarization: The Debye Model

In the case of a dispersive medium governed by a Debye model for orientational or dipolar polarization, the susceptibility kernel in (2.5) is given to be

$$g(t) = e^{-t/\tau} \frac{\epsilon_0(\epsilon_s - \epsilon_\infty)}{\tau}. \quad (2.6)$$

Such a Debye model can be represented in (macroscopic) differential form [26] as

$$\tau \frac{\partial \mathbf{P}}{\partial t} + \mathbf{P} = \epsilon_0(\epsilon_s - \epsilon_\infty) \mathbf{E}, \quad (2.7a)$$

Debye Model 1:

$$\mathbf{D} = \epsilon_0 \epsilon_\infty \mathbf{E} + \mathbf{P}, \quad (2.7b)$$

with a first order evolution equation for the polarization vector \mathbf{P} driven by the electric field. Alternatively, rewriting (2.7b) as $\mathbf{P} = \mathbf{D} - \epsilon_0 \epsilon_\infty \mathbf{E}$, the Debye model can be represented by a first order differential equation for the electric field \mathbf{E} , in terms of the electric flux density \mathbf{D} [23], given as

$$\text{Debye Model 2:} \quad \epsilon_0 \epsilon_\infty \tau \frac{\partial \mathbf{E}}{\partial t} + \epsilon_0 \epsilon_s \mathbf{E} = \tau \frac{\partial \mathbf{D}}{\partial t} + \mathbf{D}. \quad (2.8)$$

In equations (2.6), (2.7a) and (2.8), the parameter ϵ_s is the static relative permittivity.

The difference between these permittivities is commonly written $\epsilon_d := \epsilon_s - \epsilon_\infty$. The presence of instantaneous polarization is accounted for by the coefficient $\epsilon_r = \epsilon_\infty$, the infinite frequency permittivity, in the electric flux equation (2.4). The electric polarization, less the part included in the instantaneous polarization, is seen to be a decaying exponential with relaxation parameter τ , which is driven by the electric field. This model was first proposed by Debye [17] to model the behavior of materials that possess permanent dipole moments. The magnitude of the polarization term \mathbf{P} represents the degree of alignment of these individual moments and is based on a uniformity assumption at the molecular level (see [7]). The choice of coefficients in (2.7a) gives a physical interpretation to ϵ_s and ϵ_∞ as the relative permittivities of the medium in the limit of the static field and very high frequencies, respectively [6]. In the static case, we have $\mathbf{P}_t = \mathbf{0}$, so that $\mathbf{P} = \epsilon_0(\epsilon_s - \epsilon_\infty)\mathbf{E}$ and $\mathbf{D} = \epsilon_0\epsilon_s\mathbf{E}$. For very high frequencies, $\tau\mathbf{P}_t$ dominates \mathbf{P} so that $\mathbf{P} \approx 0$ and $\mathbf{D} = \epsilon_0\epsilon_\infty\mathbf{E}$ (thus the notation of ∞).

Biological cells and tissues display very high values of the dielectric constants at low frequencies, and these values decrease in almost distinct steps as the excitation frequency is increased. The Debye model is most often used to model electromagnetic wave interactions with water-based substances, such as biological materials. In particular, biological tissue is well represented by multi-pole Debye models, by accounting for permanent dipole moments in the water. The Debye model has other physical characteristics which make it attractive from an analytical point of view (for details, see [48]). Additionally, very efficient numerical methods exist for the Debye model, thus it is very common for linear combinations of Debye models to be used to approximate more complex polarization mechanisms.

2.2 Electronic Polarization: The Lorentz Model

For the Lorentz model for electronic polarization the susceptibility kernel in (2.5) is given to be

$$g(t) = e^{-\nu t/2} \sin(\nu_0 t) \frac{\epsilon_0 \omega_p^2}{\nu_0}. \quad (2.9)$$

In (2.9), the *plasma frequency* ω_p is defined as $\omega_p = \omega_0 \sqrt{\epsilon_d}$ where again $\epsilon_d = \epsilon_s - \epsilon_\infty$ with ϵ_s and ϵ_∞ as defined for the Debye model. The parameter ω_0 is the resonance frequency of the material while the parameter ν is a damping coefficient. In (2.9), the parameter ν_0 is defined as

$$\nu_0 = \sqrt{\omega_0^2 - \frac{\nu^2}{4}}.$$

The Lorentz model is formulated by modeling the atomic structure of the material as a damped vibrating system representing a deformable electron cloud at the atomic level [6]. Applying classical Newtonian laws of motion, we find that the displacement of the outermost shell of the atom satisfies a second-order ordinary differential equation [48] and thus, a Lorentz model can be represented in (macroscopic) differential form [6] as

$$\frac{\partial^2 \mathbf{P}}{\partial t^2} + \nu \frac{\partial \mathbf{P}}{\partial t} + \omega_0^2 \mathbf{P} = \epsilon_0 \omega_p^2 \mathbf{E}, \quad (2.10a)$$

Lorentz Model 1:

$$\mathbf{D} = \epsilon_0 \epsilon_\infty \mathbf{E} + \mathbf{P}, \quad (2.10b)$$

with a second order evolution equation for the polarization vector \mathbf{P} driven by the electric field. Alternatively, rewriting (2.10b) as $\mathbf{P} = \mathbf{D} - \epsilon_0 \epsilon_\infty \mathbf{E}$, the Lorentz model can be represented by a second order differential equation for the electric field \mathbf{E} , in terms of the electric flux density \mathbf{D} [23], given as

$$\text{Lorentz Model 2:} \quad \epsilon_0 \epsilon_\infty \frac{\partial^2 \mathbf{E}}{\partial t^2} + \epsilon_0 \epsilon_\infty \nu \frac{\partial \mathbf{E}}{\partial t} + \epsilon_0 \epsilon_s \omega_0^2 \mathbf{E} = \frac{\partial^2 \mathbf{D}}{\partial t^2} + \nu \frac{\partial \mathbf{D}}{\partial t} + \omega_0^2 \mathbf{D}. \quad (2.11)$$

Another alternative to representing a Lorentz material is to rewrite (2.10a) as a system of first order equations [25] by defining $\frac{\partial \mathbf{P}}{\partial t} = \mathbf{J}$ along with the constitutive law (2.10b) as

$$\frac{\partial \mathbf{P}}{\partial t} = \mathbf{J}, \quad (2.12a)$$

$$\text{Lorentz Model 3:} \quad \frac{\partial \mathbf{J}}{\partial t} + \nu \mathbf{J} + \omega_0^2 \mathbf{P} = \epsilon_0 \omega_p^2 \mathbf{E}, \quad (2.12b)$$

$$\mathbf{D} = \epsilon_0 \epsilon_\infty \mathbf{E} + \mathbf{P}. \quad (2.12c)$$

3 Reduction to One Dimension

We consider the one dimensional case in which the electric field is assumed to be polarized to have oscillations in the x - z plane such that it oscillates in the x direction and propagates in the z direction.

For any field vector $\mathbf{V}(t, \mathbf{x})$, we can write

$$\mathbf{V}(t, \mathbf{x}) = \hat{e}_d V(t, z), \quad (3.1)$$

where \hat{e}_d is a unit vector in the d direction, and $V(t, z)$ is a scalar function of t and z . If $\mathbf{V} = \mathbf{E}, \mathbf{D}, \mathbf{P}, \mathbf{J}$, or \mathbf{J}_s , then $d = x$ as all these field quantities oscillate in the x direction. If $\mathbf{V} = \mathbf{H}$, or \mathbf{B} , then $d = y$ as the magnetic field and flux oscillate in the y direction. All the fields propagate in the z direction. Thus, we are only concerned with the scalar values $E(t, z)$, $H(t, z)$, $D(t, z)$, $B(t, z)$, $P(t, z)$, $J(t, z)$, and $J_s(t, z)$.

In this case Maxwell's equations (2.1) in the interior of the domain Ω become

$$\frac{\partial B}{\partial t} = \frac{\partial E}{\partial z}, \quad (3.2a)$$

$$\frac{\partial D}{\partial t} + J_s = \frac{1}{\mu_0} \frac{\partial B}{\partial z}. \quad (3.2b)$$

Using the constitutive law (2.7b) (also (2.10b)) in 1D, i.e.,

$$D = \epsilon_0 \epsilon_\infty E + P. \quad (3.3)$$

we can rewrite Ampère's law (3.2b) as

$$\epsilon_0 \epsilon_\infty \frac{\partial E}{\partial t} + \frac{\partial P}{\partial t} + J_s = \frac{1}{\mu_0} \frac{\partial B}{\partial z} \quad (3.4)$$

4 $2M$ Order Spatial Approximations

In this section we describe the construction of higher order spatial approximations to Maxwell's equations in 1D described in Section 2. This entails the construction of higher order spatial approximations to the first order derivative operator $\partial/\partial z$. The construction presented in this section uses the notation from [14, 4] and is similar to an analogous construction performed for the Laplace operator in [4].

4.1 Staggered ℓ^2 Normed Spaces

Following the notation in [14, p. 36], we introduce the following staggered ℓ^2 normed spaces that will aid in obtaining the basic properties of the high order approximations. We define the *primary grid* of \mathbb{R} with space step size h to be

$$G_p = \{\ell h \mid \ell \in \mathbb{Z}\}, \quad (4.1)$$

and the *dual grid* of \mathbb{R} with space step size h to be

$$G_d = \left\{ \left(\ell + \frac{1}{2} \right) h \mid \ell \in \mathbb{Z} \right\}. \quad (4.2)$$

For any function v , we denote $v_\ell = v(\ell h)$ and $v_{\ell+\frac{1}{2}} = v((\ell + \frac{1}{2})h)$. We define staggered ℓ^2 normed spaces on G_p and G_d , respectively, as

$$V_0 = \{(v_\ell), \ell \in \mathbb{Z} \mid h \sum_{\ell \in \mathbb{Z}} |v_\ell|^2 \leq \infty\},$$

$$V_{\frac{1}{2}} = \{(v_{\ell+\frac{1}{2}}), \ell \in \mathbb{Z} \mid h \sum_{\ell \in \mathbb{Z}} |v_{\ell+\frac{1}{2}}|^2 \leq \infty\},$$

with scalar products $(\cdot, \cdot)_0$ and $(\cdot, \cdot)_{\frac{1}{2}}$ derived from the norms $\|v\|_0^2 = h \sum |v_\ell|^2$ and $\|v\|_{\frac{1}{2}}^2 = h \sum |v_{\ell+\frac{1}{2}}|^2$.

Next, we define the discrete operators

$$\mathcal{D}_{p,h}^{(2)} : V_0 \rightarrow V_{\frac{1}{2}} \text{ defined by } \left(\mathcal{D}_{p,h}^{(2)} u \right)_{\ell+\frac{1}{2}} = \frac{u_{\ell+p} - u_{\ell-p+1}}{(2p-1)h},$$

$$\tilde{\mathcal{D}}_{p,h}^{(2)} : V_{\frac{1}{2}} \rightarrow V_0 \text{ defined by } \left(\tilde{\mathcal{D}}_{p,h}^{(2)} u \right)_\ell = \frac{u_{\ell+p-\frac{1}{2}} - u_{\ell-p+\frac{1}{2}}}{(2p-1)h}.$$

These are second-order discrete approximations of the operator $\partial/\partial z$ computed with stepsize $(2p-1)h$.

Remark 4.1 If we denote \mathcal{D}^* to be the adjoint of the discrete operator \mathcal{D} for the ℓ^2 scalar product, we can note that $\tilde{\mathcal{D}}_{p,h}^{(2)} = -\left(\mathcal{D}_{p,h}^{(2)}\right)^*$, (c.f. [14, p. 37]).

If $u \in C^{2m+3}(\mathbf{R})$, with m an integer, and $m \geq 1$, we have [14, p. 53]

$$\left(\tilde{\mathcal{D}}_{1,h}^{(2)}u\right)_\ell = \frac{\partial u_\ell}{\partial z} + \sum_{i=1}^m \frac{h^{2i}}{(2i+1)!2^{2i}} \frac{\partial^{2i+1}u_\ell}{\partial z^{2i+1}} + \mathcal{O}(h^{2m+2}), \quad (4.3)$$

using the Taylor expansion of $\tilde{\mathcal{D}}_{1,h}^{(2)}$ at $z = \ell h$. Similarly, using the Taylor expansion of $\mathcal{D}_{1,h}^{(2)}$ at $z = \ell h$ we have

$$\left(\mathcal{D}_{1,h}^{(2)}u\right)_{\ell+\frac{1}{2}} = \frac{\partial u_{\ell+\frac{1}{2}}}{\partial z} + \sum_{i=1}^m \frac{h^{2i}}{(2i+1)!2^{2i}} \frac{\partial^{2i+1}u_{\ell+\frac{1}{2}}}{\partial z^{2i+1}} + \mathcal{O}(h^{2m+2}). \quad (4.4)$$

4.2 Two Different Ways of Constructing Finite Difference Approximations

Following the work done in [4], we construct finite difference approximations of order $2M$ of the first order operator $\partial/\partial z$, where $M \in \mathbb{N}$ is arbitrary. These approximations will be denoted as

$$\begin{aligned} \mathcal{D}_{1,h}^{(2M)} &: V_0 \rightarrow V_{\frac{1}{2}}, \\ \tilde{\mathcal{D}}_{1,h}^{(2M)} &: V_{\frac{1}{2}} \rightarrow V_0. \end{aligned}$$

The operators $\mathcal{D}_{1,h}^{(2M)}$ and $\tilde{\mathcal{D}}_{1,h}^{(2M)}$ can be considered from two different points of view, namely

- (V1) As linear combinations of second order approximations to $\partial/\partial z$ computed with different space steps, and
- (V2) As a result of the truncation of an appropriate series expansion of the symbol of the operator $\partial/\partial z$.

In [4], these two viewpoints were adopted for construction of finite difference approximations to the Laplace operator.

4.2.1 Linear Combinations of Second Order Approximations to $\partial/\partial z$

In the case of (V1), if we consider the linear combinations

$$\mathcal{D}_{1,h}^{(2M)} = \sum_{p=1}^M \lambda_{2p-1}^{2M} \mathcal{D}_{p,h}^{(2)}, \quad (4.5)$$

$$\tilde{\mathcal{D}}_{1,h}^{(2M)} = \sum_{p=1}^M \lambda_{2p-1}^{2M} \tilde{\mathcal{D}}_{p,h}^{(2)}, \quad (4.6)$$

then by replacing $h/2$ by $(2p-1)h/2$ in (4.3) and by inserting the different Taylor expansions obtained from (4.3) into (4.6) with $m = M - 1$ we obtain ([14, p. 53])

$$\begin{aligned} \left(\tilde{\mathcal{D}}_{1,h}^{(2M)}u\right)_\ell &= \sum_{p=1}^M \lambda_{2p-1}^{2M} \sum_{i=0}^{M-1} \left[\left(\frac{(2p-1)h}{2}\right)^{2i} \frac{1}{(2i+1)!} \frac{\partial^{2i+1}u_\ell}{\partial z^{2i+1}} + \mathcal{O}(h^{2M}) \right] \\ &= \sum_{i=0}^{M-1} \left[\frac{h^{2i}}{2^{2i}(2i+1)!} \frac{\partial^{2i+1}u_\ell}{\partial z^{2i+1}} \sum_{p=1}^M \lambda_{2p-1}^{2M} (2p-1)^{2i} \right] + \mathcal{O}(h^{2M}). \end{aligned} \quad (4.7)$$

Requiring $\left(\tilde{\mathcal{D}}_{1,h}^{(2M)}u\right)_\ell$ to approximate $\partial u_\ell/\partial z$ with error $\mathcal{O}(h^{2M})$ leads to the following system of equations in the λ 's

$$\begin{array}{ccccccc} \lambda_1^{2M} & +\lambda_3^{2M} & +\lambda_5^{2M} & +\dots & +\lambda_{2M-1}^{2M} & & = 1 \\ \lambda_1^{2M} & +3^2\lambda_3^{2M} & +5^2\lambda_5^{2M} & +\dots & +(2M-1)^2\lambda_{2M-1}^{2M} & & = 0 \\ \lambda_1^{2M} & +3^4\lambda_3^{2M} & +5^4\lambda_5^{2M} & +\dots & +(2M-1)^4\lambda_{2M-1}^{2M} & & = 0 \\ \vdots & \vdots & \vdots & \vdots & \vdots & & \vdots \\ \lambda_1^{2M} & +3^{2M-2}\lambda_3^{2M} & +5^{2M-2}\lambda_5^{2M} & +\dots & +(2M-1)^{2M-2}\lambda_{2M-1}^{2M} & & = 0 \end{array} \quad (4.8)$$

Following the approach in [4] we can derive explicit formulas for the λ 's. First we rewrite system (4.8) in matrix form as

$$\begin{pmatrix} 1^0 & 3^0 & 5^0 & \dots & (2M-1)^0 \\ 1^2 & 3^2 & 5^2 & \dots & (2M-1)^2 \\ 1^4 & 3^4 & 5^4 & \dots & (2M-1)^4 \\ \vdots & \vdots & \vdots & \vdots & \vdots \\ 1^{2M-2} & 3^{2M-2} & 5^{2M-2} & \dots & (2M-1)^{2M-2} \end{pmatrix} \begin{pmatrix} \lambda_1^{2M} \\ \lambda_3^{2M} \\ \lambda_5^{2M} \\ \vdots \\ \lambda_{2M-1}^{2M} \end{pmatrix} = \begin{pmatrix} 1 \\ 0 \\ 0 \\ \vdots \\ 0 \end{pmatrix}. \quad (4.9)$$

Next we define $\forall n \in \mathbb{Z}$, the double factorial as

$$n!! = \begin{cases} n \cdot (n-2) \cdot (n-4) \dots 5 \cdot 3 \cdot 1 & n > 0, \text{ odd} \\ n \cdot (n-2) \cdot (n-4) \dots 6 \cdot 4 \cdot 2 & n > 0, \text{ even} \\ 1, & n = -1, 0. \end{cases} \quad (4.10)$$

Theorem 4.1 *For any $M \in \mathbb{N}$, the coefficients λ_{2p-1}^{2M} of system (4.9) are given by the explicit formula*

$$\lambda_{2p-1}^{2M} = \frac{2(-1)^{p-1}[(2M-1)!!]^2}{(2M+2p-2)!!(2M-2p)!!(2p-1)}, \quad (4.11)$$

where $1 \leq p \leq M$.

Proof. The proof here is the analogue of the proof of Theorem 1.1 in [4] for our case. Let us denote the matrix of system (4.9) as W_{2M} . We define the vector $\lambda^{2M} = (\lambda_1^{2M}, \lambda_3^{2M}, \lambda_5^{2M}, \dots, \lambda_{2M-1}^{2M})^T$. Multiplying the linear system of equations in (4.9) by any vector $u = (u_1, u_2, \dots, u_M)^T \in \mathbb{R}^M$, we get the equation

$$u^T W_{2M} \lambda^{2M} = u_1. \quad (4.12)$$

Next, we define the even polynomial of degree $2M - 2$ associated to the vector u as

$$P_u(x) = u_1 + u_2(2x - 1)^2 + u_3(2x - 1)^4 + \dots + u_M(2x - 1)^{2M-2}, \quad (4.13)$$

from which we obtain the equation

$$u^T W_{2M} = (P_u(1), P_u(2), P_u(3), \dots, P_u(M)), \quad (4.14)$$

which permits rewriting equation (4.12) as

$$\sum_{j=1}^M P_u(j) \lambda_{2j-1}^{2M} = P_u\left(\frac{1}{2}\right). \quad (4.15)$$

Satisfying equation (4.12) $\forall u \in \mathbb{R}^M$ is equivalent to having equation (4.15) hold for any polynomial $P \in \mathcal{P}[\mathbb{R}]$ which is even and of degree $2M - 2$.

We now consider the polynomials

$$Q_p(x) = \prod_{1 \leq r \leq M, r \neq p} \left(1 - \frac{(2x - 1)^2}{(2r - 1)^2}\right) \quad (4.16)$$

which, for each integer $1 \leq p \leq M$ are even and of degree $2M - 2$. We note that $Q_p(x)$ vanishes at $x = 1, 2, 3, \dots, M$ except at $x = p$. Using $P = Q_p$ in (4.15) we have

$$Q_p(p) \lambda_{2p-1}^{2M} = Q_p\left(\frac{1}{2}\right) = 1,$$

which implies that

$$\lambda_{2p-1}^{2M} = \frac{1}{Q_p(p)} = \prod_{1 \leq r \leq M, r \neq p} \left(1 - \frac{(2p - 1)^2}{(2r - 1)^2}\right)^{-1}. \quad (4.17)$$

We require the following identities (given without proof)

$$\prod_{1 \leq r \leq M, r \neq p} \left(1 + \frac{(2p - 1)}{(2r - 1)}\right)^{-1} = \frac{2^p(p - 1)!(2M - 1)!!}{(2M + 2p - 2)!!}, \quad (4.18)$$

and

$$\prod_{1 \leq r \leq M, r \neq p} \left(1 - \frac{(2p - 1)}{(2r - 1)}\right)^{-1} = \frac{(-1)^{p-1}(2M - 1)!!}{2^{p-1}(2M - 2p)!!(2p - 1)(p - 1)!}, \quad (4.19)$$

where $p \in \mathbb{Z}, 1 \leq p \leq M$. From equations (4.17), (4.18) and (4.19) we can easily obtain the explicit formula (4.11).

■

Remark 4.2 *The result in (4.11) has been obtained, using other techniques, by other authors in the past, see [19, 21, 20]. In [4], the authors prove several additional properties of the corresponding coefficients for higher order approximations of the Laplace operator. Similar properties for the coefficients λ_{2p-1}^{2M} can be proved. Some of these properties have been proved in [21, 20].*

4.2.2 Series Expansion of the Symbol of the Operator $\partial/\partial z$

With respect to the second point of view, (V2), we can interpret the operators $\mathcal{D}_{1,h}^{(2M)}$ and $\tilde{\mathcal{D}}_{1,h}^{(2M)}$ via their *symbols* (c.f., [4]). We define the symbol of a differential operator, as well as its finite difference approximation, via its application to harmonic plane waves. Thus, if $v(z) = e^{ikz}$ then $\partial v/\partial z = ikv(z)$, and

$$\mathcal{F}(\partial/\partial z) = ik, \quad (4.20)$$

where $\mathcal{F}(\partial/\partial z)$ denotes the symbol of the differential operator $\partial/\partial z$. In a similar fashion, we can show that the symbol of the finite difference operator $\tilde{\mathcal{D}}_{1,h}^{(2M)}$ can be written as

$$\mathcal{F}\left(\tilde{\mathcal{D}}_{1,h}^{(2M)}\right) = \frac{2i}{h} \sum_{j=1}^M \frac{\lambda_{2j-1}^{2M}}{2j-1} \sin(kh(2j-1)/2). \quad (4.21)$$

We now introduce the following alternative formulation to the symbol of the operator $\tilde{\mathcal{D}}_{1,h}^{(2M)}$.

Theorem 4.2 *The symbol of the operator $\tilde{\mathcal{D}}_{1,h}^{(2M)}$ can be rewritten in the form*

$$\mathcal{F}\left(\tilde{\mathcal{D}}_{1,h}^{(2M)}\right) = \frac{2i}{h} \sum_{p=1}^M \gamma_{2p-1} \sin^{2p-1}(kh/2), \quad (4.22)$$

where the coefficients γ_{2p-1} are strictly positive, independent of M , and are given by the explicit formula

$$\gamma_{2p-1} = \frac{[(2p-3)!!]^2}{(2p-1)!}. \quad (4.23)$$

Proof. We again follow an analogous proof in [4] for approximations of the Laplace operator. Let us define $K := kh/2$. Since $\tilde{\mathcal{D}}_{1,h}^{(2M)}$ is of order $2M$ the difference in the symbols of $\partial/\partial z$ and the symbol of $\tilde{\mathcal{D}}_{1,h}^{(2M)}$ must be of $\mathcal{O}(K^{2M+1})$ for small K . Thus, we have

$$\mathcal{F}\left(\frac{\partial}{\partial z}\right) = ik = \frac{2iK}{h} = \frac{2i}{h} \left(\sum_{p=1}^M \gamma_{2p-1} \sin^{2p-1} K \right) + \mathcal{O}(K^{2M+1}). \quad (4.24)$$

This implies that the γ_{2p-1} are the first M coefficients of a series expansion of K in terms of $\sin K$. Set $x = \sin K$ for $|K| < \pi/2$. Then, $K = \sin^{-1} x$, $x \in (-1, 1)$ with

$$\sin^{-1} x = \sum_{p=1}^M \gamma_{2p-1} x^{2p-1} + \mathcal{O}(x^{2M+2}). \quad (4.25)$$

Requiring that equation (4.25) be true $\forall M \in \mathbb{N}$ implies that if a solution exists for $\{\gamma_{2p-1}\}_{p=1}^M$, then it is unique. We note that the function $Y(x) = \sin^{-1} x$ obeys the differential equation

$$(1-x^2)Y'' - xY' = 0, \quad x \in (-1, 1) \quad (4.26)$$

with the conditions

$$Y(0) = 0, Y'(0) = 1. \quad (4.27)$$

Substituting, formally, the series expansion $Y(x) = \sum_{p=1}^{\infty} \gamma_{2p-1} x^{2p-1}$ into (4.26) we obtain the following equation

$$(6\gamma_3 - \gamma_1) + \sum_{p=2}^{\infty} \beta_{2p-1} x^{2p-1} = 0, \quad (4.28)$$

where

$$\beta_{2p-1} = (2p+1)(2p)\gamma_{2p+1} - (2p-1)^2\gamma_{2p-1}. \quad (4.29)$$

This implies that

$$\gamma_3 = \frac{1}{6}\gamma_1, \quad (4.30)$$

and

$$\gamma_{2p+1} = \frac{(2p-1)^2}{(2p)(2p+1)}\gamma_{2p-1}, \quad (4.31)$$

which gives us the formula

$$\gamma_{2p-1} = \frac{[(2p-3)!!]^2}{(2p-1)!}\gamma_1. \quad (4.32)$$

From the conditions (4.27) we see that $\gamma_1 = 1$, so that we finally obtain the formula (4.23).
■

Remark 4.3 We note that the relation (4.31) gives

$$\lim_{p \rightarrow \infty} \frac{\gamma_{2p+1}}{\gamma_{2p-1}} = 1. \quad (4.33)$$

This justifies the term by term differentiation of the series expansion of Y on $(-1, 1)$ in the proof of Theorem 4.2.

Remark 4.4 To our knowledge the result obtained in Theorem 4.2 is new and has not been proved elsewhere. It is this result that is key to obtaining closed form analytical stability and dispersion formulae for the $(2, 2M)$ finite difference methods that we consider in Section 5. The stability and dispersion analysis, based on Theorem 4.2, will be performed in Section 6, and Section 7, respectively.

Remark 4.5 We note that the coefficients γ_{2p-1} , defined in (4.23), are the coefficients in the Taylor expansion of the function $\sin^{-1} x$ around zero.

Lemma 4.1 The series $\sum_{p=1}^{\infty} \gamma_{2p-1} x^{2p-1}$ is convergent and its sum is $\pi/2$.

Proof. From the proof of Theorem 4.2 we have

$$\sum_{p=1}^{\infty} \gamma_{2p-1} x^{2p-1} = \sin^{-1} x, \quad \forall x \in (-1, 1). \quad (4.34)$$

Consider $M \in \mathbb{N}$. From the positivity of the γ_{2p-1} coefficients, we have

$$\sum_{p=1}^M \gamma_{2p-1} x^{2p-1} < \sin^{-1} x. \quad (4.35)$$

Letting $x \rightarrow 1$ in both sides of the inequality (4.35) we obtain

$$\sum_{p=1}^M \gamma_{2p-1} \leq \frac{\pi}{2}. \quad (4.36)$$

Next, allowing $M \rightarrow \infty$ in the inequality

$$\sum_{p=1}^M \gamma_{2p-1} x^{2p-1} < \sum_{p=1}^M \gamma_{2p-1}, \quad (4.37)$$

gives the the inequality

$$\sin^{-1} x = \sum_{p=1}^{\infty} \gamma_{2p-1} x^{2p-1} \leq \sum_{p=1}^{\infty} \gamma_{2p-1}, \quad (4.38)$$

$\forall x \in (-1, 1)$. Now letting $x \rightarrow 1$ in (4.38) we obtain

$$\frac{\pi}{2} \leq \sum_{p=1}^{\infty} \gamma_{2p-1}. \quad (4.39)$$

Thus, the series $\sum_{p=1}^{\infty} \gamma_{2p-1}$ is bounded above and below by $\frac{\pi}{2}$. This proves the convergence of the series to $\frac{\pi}{2}$. ■

In Tables 1 and 2 we provide the coefficients λ_{2p-1}^{2M} and γ_{2p-1} , respectively, from the two different approaches for representing the $2M$ order finite difference approximation to the operator $\partial/\partial z$ for various values of M and p .

Finally, we show by direct comparison that the two different representations of the symbol of the discrete operator $\tilde{\mathcal{D}}_{1,h}^{(2M)}$, given in equations (4.21) and (4.22), with the coefficients λ_{2p-1}^{2M} , and γ_{2p-1} as defined in (4.11), and (4.23), respectively, are equivalent for all M .

Theorem 4.3 $\forall M \in \mathbb{N}$, M finite we have

$$\mathcal{F}\left(\tilde{\mathcal{D}}_{1,h}^{(2M)}\right) = \frac{2i}{h} \sum_{j=1}^M \frac{\lambda_{2j-1}^{2M}}{2j-1} \sin((2j-1)\theta) = \frac{2i}{h} \sum_{p=1}^M \gamma_{2p-1} \sin^{2p-1}(\theta), \quad (4.40)$$

where $\theta = kh/2$.

Proof. We have for integers $1 \leq j \leq M$, the identity

$$\sin((2j-1)\theta) = (-1)^{j-1} T_{2j-1}(\sin(\theta)), \quad (4.41)$$

Table 1: Coefficients λ_{2p-1}^{2M} for approximations from 2nd order to 8th order

2M	λ_1^{2M}	λ_3^{2M}	λ_5^{2M}	λ_7^{2M}
2	1			
4	$\frac{9}{8}$	$-\frac{1}{8}$		
6	$\frac{75}{64}$	$-\frac{25}{128}$	$\frac{3}{128}$	
8	$\frac{1225}{1024}$	$-\frac{245}{1024}$	$\frac{49}{1024}$	$-\frac{5}{1024}$

Table 2: The first four coefficients γ_{2p-1}

γ_1	γ_3	γ_5	γ_7
1	$\frac{1}{6}$	$\frac{3}{40}$	$\frac{5}{112}$

where T_{2j-1} are the Chebyshev polynomials of degree $2j - 1$. Using properties of these polynomials we can rewrite the right hand side of (4.41) as

$$\sin((2j - 1)\theta) = \sum_{p=1}^j \alpha_p^j \sin^{2p-1}(\theta), \quad (4.42)$$

where for $1 \leq p \leq j$, the coefficients α_p^j in equation (4.42) are given as

$$\alpha_p^j = (-1)^{2j-p-1} \binom{2j-1}{j+p-1} \binom{(j+p-1)!}{(j-p)!} \frac{2^{2p-2}}{(2p-1)!}. \quad (4.43)$$

Substituting (4.42) into the representation (4.21) of the symbol of the operator $\tilde{\mathcal{D}}_{1,h}^{(2M)}$ we have

$$\mathcal{F}\left(\tilde{\mathcal{D}}_{1,h}^{(2M)}\right) = \frac{2i}{h} \sum_{j=1}^M \frac{\lambda_{2j-1}^{2M}}{2j-1} \sin((2j-1)\theta) \quad (4.44)$$

$$= \frac{2i}{h} \sum_{j=1}^M \frac{\lambda_{2j-1}^{2M}}{2j-1} \sum_{p=1}^j \alpha_p^j \sin^{2p-1}(\theta). \quad (4.45)$$

Rearranging terms in equation (4.45) we have

$$\mathcal{F}\left(\tilde{\mathcal{D}}_{1,h}^{(2M)}\right) = \frac{2i}{h} \sum_{p=1}^M \left(\sum_{j=p}^M \frac{\lambda_{2j-1}^{2M}}{2j-1} \alpha_p^j \right) \sin^{2p-1}(\theta). \quad (4.46)$$

Using the formulae (4.11) and (4.43), the coefficients in the expansion (4.46) can be written out as

$$\sum_{j=p}^M \frac{\lambda_{2j-1}^{2M}}{2j-1} \alpha_p^j = \sum_{j=p}^M \frac{(-1)^{3j-p-2} (j+p-2)! [(2M-1)!!]^2 2^{2p-1}}{(2p-1)! (j-p)! (2j-1) (2M-2j)! (2M+2j-2)!}. \quad (4.47)$$

Changing the summation index to $k = j - p$ in (4.47), and simplifying terms using the property of the double factorial, $(2n)!! = 2^n n!$, we get

$$\sum_{j=p}^M \frac{\lambda_{2j-1}^{2M}}{2j-1} \alpha_p^j = \frac{[(2M-1)!!]^2 2^{2p}}{2^{2M} (2p-1)!} \sum_{k=0}^{M-p} \frac{(-1)^k (2p+k-2)!}{k! (2k+2p-1) (M-p-k)! (M+k+p-1)!}. \quad (4.48)$$

We note the following useful result

$$\sum_{k=0}^{M-p} \frac{(-1)^k (2p+k-2)!}{k! (2k+2p-1) (M-p-k)! (M+k+p-1)!} = \frac{[\Gamma(p-\frac{1}{2})]^2}{4 [\Gamma(M+\frac{1}{2})]^2} \quad (4.49)$$

which can be shown using representations of the Gamma function in terms of hypergeometric functions, or verified via computer algebra software such as MAPLE. We also employ the following identities for $n \in \mathbb{Z}$

$$\Gamma(n+1) = n\Gamma(n), \quad (4.50)$$

$$\Gamma\left(n + \frac{1}{2}\right) = \frac{(2n-1)!! \sqrt{\pi}}{2^n}. \quad (4.51)$$

Substituting in (4.49) and applying as necessary (4.50) and (4.51), the summation in (4.48) reduces as follows

$$\begin{aligned} \sum_{j=p}^M \frac{\lambda_{2j-1}^{2M}}{2j-1} \alpha_p^j &= \frac{[(2M-1)!!]^2 2^{2p}}{2^{2M} (2p-1)!} \frac{[\Gamma(p-\frac{1}{2})]^2}{4 [\Gamma(M+\frac{1}{2})]^2} \\ &= \frac{[(2p-3)!!]^2}{(2p-1)!} \\ &= \gamma_{2p-1}, \text{ as given in (4.23)}. \end{aligned} \quad (4.52)$$

Thus, using (4.52) in (4.46) we finally get the result (4.40). ■

5 High Order Numerical Methods for Dispersive Media

In this section we study a family of finite difference schemes for Maxwell's equations in Debye and Lorentz dispersive media in 1D. These schemes are based on the discrete higher order $(2M, M \in \mathbb{N})$ approximations to the first order operator that were constructed in Section 4. For the time discretization we employ the standard leap-frog scheme which is second order

accurate in time. We will denote the resulting schemes as $(2, 2M)$ schemes. When $M = 2$, the corresponding $(2, 2)$ schemes are extensions of the famous Yee scheme or FDTD scheme for Maxwell's equations to dispersive media.

Let us denote the time step by $\Delta t > 0$ and the spatial mesh step size by $h = \Delta z > 0$. The nodes of the primary spatial mesh will be denoted by $z_j = j\Delta z$, $j \in \mathbb{Z}$, while the nodes of the dual spatial mesh will be denoted by $z_{j+\frac{1}{2}} = (j + \frac{1}{2})\Delta z$, $j \in \mathbb{Z}$. The nodes of the primary temporal mesh will be denoted by $t^n = n\Delta t$, $n \in \mathbb{N}$, while the nodes of the dual temporal mesh will be denoted by $t^{n+\frac{1}{2}} = (n + \frac{1}{2})\Delta t$, $n \in \mathbb{N}$. The discrete solution will be computed at these spatial and temporal nodes (either both primary or both dual) in the space-time mesh. For any field variable $V(t, z)$, we denote the approximation of $V(t^n, z_j)$ by V_j^n on the primary space-time mesh, and the approximation of $V(t^{n+\frac{1}{2}}, z_{j+\frac{1}{2}})$ by $V_{j+\frac{1}{2}}^{n+\frac{1}{2}}$ on the dual space-time mesh.

With the above notation, the $(2, 2M)$ discretized equations for Maxwell's equations (3.2a) and (3.2b), respectively, in 1D (with $J_s = 0$) are

$$\frac{B_{j+\frac{1}{2}}^{n+\frac{1}{2}} - B_{j+\frac{1}{2}}^{n-\frac{1}{2}}}{\Delta t} = \sum_{p=1}^M \frac{\lambda_{2p-1}^{2M}}{2p-1} \left(\frac{E_{j+p}^n - E_{j-p+1}^n}{\Delta z} \right), \quad (5.1a)$$

$$\frac{D_j^{n+1} - D_j^n}{\Delta t} = \frac{1}{\mu_0} \sum_{p=1}^M \frac{\lambda_{2p-1}^{2M}}{2p-1} \left(\frac{B_{j+p-\frac{1}{2}}^{n+\frac{1}{2}} - B_{j-p+\frac{1}{2}}^{n+\frac{1}{2}}}{\Delta z} \right), \quad (5.1b)$$

where, λ_{2p-1}^{2M} is defined in (4.11). Alternatively, discretizing (3.2a) with (3.4) we have the discrete system

$$\frac{B_{j+\frac{1}{2}}^{n+\frac{1}{2}} - B_{j+\frac{1}{2}}^{n-\frac{1}{2}}}{\Delta t} = \sum_{p=1}^M \frac{\lambda_{2p-1}^{2M}}{2p-1} \left(\frac{E_{j+p}^n - E_{j-p+1}^n}{\Delta z} \right), \quad (5.2a)$$

$$\epsilon_0 \epsilon_\infty \frac{E_j^{n+1} - E_j^n}{\Delta t} = \frac{1}{\mu_0} \sum_{p=1}^M \frac{\lambda_{2p-1}^{2M}}{2p-1} \left(\frac{B_{j+p-\frac{1}{2}}^{n+\frac{1}{2}} - B_{j-p+\frac{1}{2}}^{n+\frac{1}{2}}}{\Delta z} \right) - \frac{P_j^{n+1} - P_j^n}{\Delta t}. \quad (5.2b)$$

In (5.1b) (respectively, (5.2b)), the electric flux density D (respectively, the polarization P) will be determined by the polarization model.

5.1 $(2, 2M)$ Numerical Methods for Debye Media

For a Debye media we add the discretized (in time) version of the polarization model to the discretized system of Maxwell's equations. The system given by (5.2a) and (5.2b) is closed by the second order time discretization of (2.7a) for the polarization P , in terms of the electric field E , in the form

$$\tau \frac{P_j^{n+1} - P_j^n}{\Delta t} + \frac{P_j^{n+1} + P_j^n}{2} = \epsilon_0 \epsilon_d \frac{E_j^{n+1} + E_j^n}{2}. \quad (5.3)$$

Alternatively, we can construct $(2, 2M)$ schemes for Debye media by adding the discretized in time version of (2.8) given as

$$\epsilon_0 \epsilon_\infty \tau \frac{E_j^{n+1} - E_j^n}{\Delta t} + \epsilon_0 \epsilon_s \frac{E_j^{n+1} + E_j^n}{2} = \tau \frac{D_j^{n+1} - D_j^n}{\Delta t} + \frac{D_j^{n+1} + D_j^n}{2}, \quad (5.4)$$

to the system defined in (5.1a) and (5.1b). As shown in [31], for the $(2, 2)$ case, both these approaches yield equivalent stability and dispersion results. Thus in the following we will analyze only (5.2a) and (5.2b) with (5.3), although the methods could be applied to either formulation.

5.2 $(2, 2M)$ Numerical Methods for Lorentz Media

For Lorentz media we obtain two types of discretized $(2, 2M)$ methods, based on the discretization of either the second order differential equation for the macroscopic polarization P in (2.10a) (or equivalently the second order differential equation for E in (2.11)), or based on the discretization of the system of first order equations for the variables P and J , in (2.12a) and (2.12b), respectively.

5.2.1 $(2, 2M)$ JHT Schemes for Lorentz Media

One set of $(2, 2M)$ schemes for Lorentz media is constructed by adding the second order in time discretization of the second order differential equation for the macroscopic polarization P in (2.10a) given as

$$\frac{P_j^{n+1} - 2P_j^n + P_j^{n-1}}{\Delta t^2} + \nu \left(\frac{P_j^{n+1} - P_j^{n-1}}{2\Delta t} \right) + \omega_0^2 \left(\frac{P_j^{n+1} + P_j^n}{2} \right) = \epsilon_0 \omega_p^2 \frac{E_j^{n+1} + E_j^n}{2}, \quad (5.5)$$

to the discretized Maxwell equations in (5.2a) and (5.2b).

Equivalently, $(2, 2M)$ schemes for Lorentz media can be constructed by adding the time discretized version of the second order differential equation for E in (2.11) given as

$$\begin{aligned} \epsilon_0 \epsilon_\infty \frac{E_j^{n+1} - 2E_j^n + E_j^{n-1}}{\Delta t^2} + \nu \epsilon_0 \epsilon_\infty \left(\frac{E_j^{n+1} - E_j^{n-1}}{2\Delta t} \right) + \epsilon_0 \epsilon_s \omega_0^2 \left(\frac{E_j^{n+1} + E_j^n}{2} \right) \\ = \frac{D_j^{n+1} - 2D_j^n + D_j^{n-1}}{\Delta t^2} + \nu \left(\frac{D_j^{n+1} - D_j^{n-1}}{2\Delta t} \right) + \omega_0^2 \left(\frac{D_j^{n+1} + D_j^n}{2} \right), \end{aligned} \quad (5.6)$$

to the discretized Maxwell equations in (5.1a) and (5.1b).

As in the Debye case both of these approaches yield equivalent (with respect to stability and dispersion errors) $(2, 2M)$ schemes. We will denote either of these two approaches as $(2, 2M)$ JHT schemes after a similar $(2, 2)$ scheme considered in [23].

5.2.2 $(2, 2M)$ KF Schemes for Lorentz Media

A second set of $(2, 2M)$ schemes for Lorentz media is constructed by adding the second order in time discretization of the system of first order equations for the variables P and J , in

(2.12a) and (2.12b), respectively, given as

$$\frac{P_j^{n+1} - P_j^n}{\Delta t} = \frac{J_j^{n+1} + J_j^n}{2}, \quad (5.7)$$

$$\frac{J_j^{n+1} - J_j^n}{\Delta t} = -\nu \frac{J_j^{n+1} + J_j^n}{2} + \omega_p^2 \epsilon_0 \frac{E_j^{n+1} + E_j^n}{2} - \omega_0^2 \frac{P_j^{n+1} + P_j^n}{2}, \quad (5.8)$$

to the discretized system of Maxwell's equations in (5.2a) and (5.2b). We will denote such schemes as $(2, 2M)$ KF schemes after a similar $(2, 2)$ scheme considered in [25].

6 Stability Analysis

To determine stability conditions we use von Neumann analysis which allows us to localize roots of certain classes of polynomials [10]. We follow the approach in [10] in which the author derives stability conditions for the $(2, 2)$ (Yee) schemes applied to Debye and Lorentz dispersive media. This analysis is based on properties of Schur and von Neumann polynomials.

Stability conditions for the general $(2, 2M)$ schemes are made possible by the results presented in Section 4, in which finite difference approximations of the first order derivative operator are obtained as a result of the truncation of an appropriate series expansion of the symbol of this operator.

In performing the von Neumann analysis for the $(2, 2M)$ schemes we show that the resulting amplification matrices retain the same structure as in the $(2, 2)$ schemes in [10], albeit with a modified definition of the parameter q in [10]. We also show that these polynomials also have the same structure as those derived for the $(2, 2)$ schemes in [31]. This affords a complete stability analysis for the general case, as results from [10] can be used directly for the modified parameter q as we show below.

We refer the reader to [10] for a description of von-Neumann analysis and for the major theorems regarding properties of Schur and von Neumann polynomials that aid in the construction of stability criteria for the various finite difference schemes.

6.1 Stability Analysis for Debye Media

We consider the $(2, 2M)$ scheme for discretizing Maxwell's equations coupled with the Debye polarization model presented in the form of equations (5.1a), (5.1b) and (5.4). We rewrite these equations using the (modified) variables $c_\infty B_{j+\frac{1}{2}}^{n-\frac{1}{2}}$, E_j^n , and $\frac{1}{\epsilon_0 \epsilon_\infty} D_j^n$ to obtain the

modified system

(2, 2M)-Debye:

$$c_\infty B_{j+\frac{1}{2}}^{n+\frac{1}{2}} = c_\infty B_{j+\frac{1}{2}}^{n-\frac{1}{2}} + \eta_\infty \sum_{p=1}^M \frac{\lambda_{2p-1}^{2M}}{2p-1} (E_{j+p}^n - E_{j-p+1}^n), \quad (6.1a)$$

$$E_j^{n+1} = \left(\frac{2 - h_\tau \eta_s}{2 + h_\tau \eta_s} \right) E_j^n + \left(\frac{2 + h_\tau}{2 + h_\tau \eta_s} \right) \frac{1}{\epsilon_0 \epsilon_\infty} D_j^{n+1} - \left(\frac{2 - h_\tau}{2 + h_\tau \eta_s} \right) \frac{1}{\epsilon_0 \epsilon_\infty} D_j^n, \quad (6.1b)$$

$$\frac{1}{\epsilon_0 \epsilon_\infty} D_j^{n+1} = \frac{1}{\epsilon_0 \epsilon_\infty} D_j^n + \eta_\infty c_\infty \sum_{p=1}^M \frac{\lambda_{2p-1}^{2M}}{2p-1} \left(B_{j+p-\frac{1}{2}}^{n+\frac{1}{2}} - B_{j-p+\frac{1}{2}}^{n+\frac{1}{2}} \right). \quad (6.1c)$$

In equations (6.1a)-(6.1c), the parameters $c_\infty, \eta_\infty, h_\tau$ and η_s are defined as

$$c_\infty^2 := 1/(\epsilon_0 \mu_0 \epsilon_\infty) = c_0^2/\epsilon_\infty, \quad (6.2)$$

$$\eta_\infty := (c_\infty \Delta t)/\Delta z, \quad (6.3)$$

$$h_\tau := \Delta t/\tau, \quad (6.4)$$

$$\eta_s := \epsilon_s/\epsilon_\infty, \quad (6.5)$$

where c_0 is the speed of light in vacuum, and c_∞ is the speed of light in the Debye medium. The parameter η_∞ is the Courant (stability) number. We assume here that $\epsilon_s > \epsilon_\infty$ and $\tau > 0$.

All the models that we deal with are linear. Thus, we can analyze the models in the frequency domain. We look for plane wave solutions of (6.1a)-(6.1c) as numerically evaluated at the discrete space-time point (t^n, z_j) , or $(t^{n+1/2}, z_{j+1/2})$. We assume a spatial dependence of the form

$$B_{j+\frac{1}{2}}^{n+\frac{1}{2}} = \hat{B}^{n+\frac{1}{2}}(k) e^{ikz_{j+\frac{1}{2}}}, \quad (6.6a)$$

$$E_j^n = \hat{E}^n(k) e^{ikz_j}, \quad (6.6b)$$

$$D_j^n = \hat{D}^n(k) e^{ikz_j}, \quad (6.6c)$$

in all the field quantities, with k defined to be the wavenumber. (Equivalently, we can apply the discrete Fourier transform in space to the discrete equations (6.1a), (6.1b), and (6.1c)). Substituting the forms (6.6) into the higher order schemes (6.1a), (6.1b), and (6.1c), and canceling out common terms we obtain the following system

$$\begin{bmatrix} c_\infty \hat{B}^{n+\frac{1}{2}} \\ \hat{E}^{n+1} \\ \frac{1}{\epsilon_0 \epsilon_\infty} \hat{D}^{n+1} \end{bmatrix} = \begin{bmatrix} 1 & -\sigma & 0 \\ \left(\frac{2 + h_\tau}{2 + h_\tau \eta_s} \right) \sigma^* & \left(\frac{2(1-q) - h_\tau(\eta_s + q)}{2 + h_\tau \eta_s} \right) & \left(\frac{2h_\tau}{2 + h_\tau \eta_s} \right) \\ \sigma^* & -q & 1 \end{bmatrix} \begin{bmatrix} c_\infty \hat{B}^{n-\frac{1}{2}} \\ \hat{E}^n \\ \frac{1}{\epsilon_0 \epsilon_\infty} \hat{D}^n \end{bmatrix} \quad (6.7)$$

where the parameter σ is defined as

$$\sigma := -2i\eta_\infty \sum_{p=1}^M \gamma_{2p-1} \sin^{2p-1} \left(\frac{k\Delta z}{2} \right), \quad (6.8)$$

and $\sigma^* = -\sigma$ is the complex conjugate of σ . The parameter q is defined to be

$$q := |\sigma|^2 = \sigma\sigma^* = 4\eta_\infty^2 \left(\sum_{p=1}^M \gamma_{2p-1} \sin^{2p-1} \left(\frac{k\Delta z}{2} \right) \right)^2. \quad (6.9)$$

Here, we are using the equivalence between the two different representations of the symbol of the discrete (spatial) operator $\tilde{\mathcal{D}}_{1,h}^{(2M)}$ of order $2M$, given in Theorem 4.2. This is reflected in the presence of the term σ , as defined in (6.8), in the amplification matrix given in (6.7).

The characteristic polynomial retains the same form as in [31], except for the inclusion of the parameter q (instead of p^2 in [31]), and is given by:

$$\begin{aligned} P_{(2,2M)\text{-D}}(X) = & X^3 + \left(\frac{q\epsilon_\infty(2 + h_\tau) - (6\epsilon_\infty + h_\tau\epsilon_s)}{2\epsilon_\infty + h_\tau\epsilon_s} \right) X^2 \\ & + \left(\frac{q\epsilon_\infty(h_\tau - 2) + (6\epsilon_\infty - h_\tau\epsilon_s)}{2\epsilon_\infty + h_\tau\epsilon_s} \right) X - \left(\frac{2\epsilon_\infty - h_\tau\epsilon_s}{2\epsilon_\infty + h_\tau\epsilon_s} \right). \end{aligned} \quad (6.10)$$

We note that the characteristic polynomial (6.10) is the same as that derived in [10] (though here written in the form of those derived in [31]), except for the definition of the parameter q (defined in (6.9)). In [10], stability analysis was performed for the (2, 2) schemes only, and thus q was defined as $q = 4\eta_\infty^2 \sin^2 \left(\frac{kh}{2} \right)$ ($M = 1$ in equation (6.9)). The representation (4.22) for the symbol of $\tilde{\mathcal{D}}_{1,h}^{(2M)}$ allows us to retain the same compact form of the (2, 2) characteristic polynomial for the general (2, $2M$) schemes by using the modified definition (6.9) of the parameter q .

Now, using the results of the von-Neumann stability analysis performed in [10], we can generalize the stability analysis to the (2, $2M$) schemes. Assuming, for most practical applications, that $\epsilon_s > \epsilon_\infty$, a necessary and sufficient stability condition for the (2, $2M$) scheme in (6.1a)-(6.1c) is that $q \in (0, 4)$, for all wavenumbers, k , i.e.,

$$4\eta_\infty^2 \left(\sum_{p=1}^M \gamma_{2p-1} \sin^{2p-1} \left(\frac{k\Delta z}{2} \right) \right)^2 < 4, \quad \forall k, \quad (6.11)$$

which implies that

$$\eta_\infty \left(\sum_{p=1}^M \gamma_{2p-1} \right) < 1 \iff \eta_\infty \left(\sum_{p=1}^M \frac{[(2p-3)!!]^2}{(2p-1)!} \right) < 1. \quad (6.12)$$

For different values of M we obtain the following stability conditions

$$M = 1, \eta_\infty < 1 \iff \Delta t < \frac{\Delta z}{c_\infty}, \quad (6.13a)$$

$$M = 2, \eta_\infty \left(1 + \frac{1}{6}\right) < 1 \iff \Delta t < \frac{6\Delta z}{7c_\infty}, \quad (6.13b)$$

$$M = 3, \eta_\infty \left(1 + \frac{1}{6} + \frac{3}{40}\right) < 1 \iff \Delta t < \frac{120\Delta z}{149c_\infty}, \quad (6.13c)$$

\vdots

$$M = M, \eta_\infty \left(\sum_{p=1}^M \gamma_{2p-1}\right) < 1 \iff \Delta t < \frac{\Delta z}{\left(\sum_{p=1}^M \frac{[(2p-3)!!]^2}{(2p-1)!}\right) c_\infty}. \quad (6.13d)$$

In the limiting case (as $M \rightarrow \infty$), we may evaluate the infinite series using Lemma 4.1. Therefore,

$$M = \infty, \eta_\infty \left(\frac{\pi}{2}\right) < 1 \iff \Delta t < \frac{2\Delta z}{\pi c_\infty}. \quad (6.14)$$

The positivity of the coefficients γ_{2p-1} gives that the constraint on Δt in (6.14) is a lower bound on all constraints for any M . Therefore this constraint guarantees stability for all orders.

6.1.1 Dissipation Error for $(2, 2M)$ Schemes for Debye Media

While the stability criteria (6.13) give conditions for which the finite difference method of various orders are stable, they does not give any insight into the amount of error, specifically, dissipation error that may be exhibited by a particular order of method. We follow the procedures in [31, 5] to produce plots of the dissipation error for the schemes (6.1a)-(6.1c). To generate these plots we have assumed the following values of the physical parameters, as considered in [6] (note that these are appropriate constants for modeling water)

$$\epsilon_\infty = 1, \quad \epsilon_s = 78.2, \quad \tau = 8.1 \times 10^{-12} \text{ sec}. \quad (6.15)$$

In the left plot of Figure 1 we graph the absolute value of the largest root of (6.10), as a function of $k\Delta z$, using $h_\tau = 0.1$ for the finite difference schemes (6.1a)-(6.1c) of orders $M = 2, 4, 6, 8$ and the limiting ($M = \infty$) case with η_∞ set to the maximum stable value for each order, given in (6.13) for finite M , and in (6.14) for $M = \infty$. In the right plot we fix η_∞ to the maximum stable value for the limiting ($M = \infty$) case (i.e., each method uses the same value of η_∞ and that value is the largest for which all methods are guaranteed stable).

We can interpret $k\Delta z$ as the wave number if Δz is fixed, or as the inverse of the number of points per wavelength (N_{ppw}) if k is fixed. Using the latter interpretation, it is reasonable to assume that in most practical implementations $k\Delta z \leq 1$ for most wavenumbers of interest in the problem. We note that while the left plot suggests that the infinite order method has the least dissipation (maximum complex time eigenvalue closest to 1), this is mostly

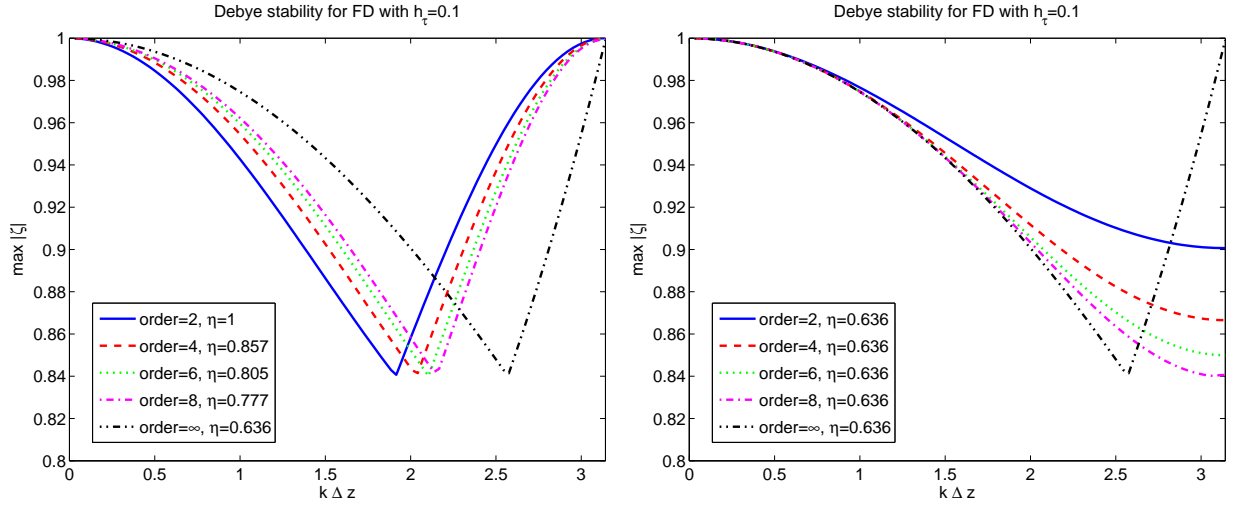


Figure 1: (Left) $\max|\zeta|$ versus $k\Delta z$ using $h_\tau = 0.1$ for the schemes (6.1a)-(6.1c) of orders $M = 2, 4, 6, 8$ and the limiting ($M = \infty$) case with η_∞ set to the maximum stable value for the order, given in (6.13) for finite M , and in (6.14) for $M = \infty$. (Right) η_∞ fixed at the maximum stable value for the limiting ($M = \infty$) case, given in (6.14).

a consequence of the severe restriction on η_∞ . It is clear in the right plot that, with all material and discretization parameters held fixed at equivalent values for all orders of the finite difference method, the second order method exhibits the least dissipation over a broad range of wave numbers.

For each of the curves in both plots of Figure 1, the maximum dissipation error (defined here to be $1 - \max|\zeta|$) is unacceptably high with a value ($1 - \max|\zeta|$) between 0.1 and 0.2. The dissipation error of the numerical schemes can be reduced by decreasing h_τ . Note that we are assuming the time step Δt is determined by the choice of h_τ and the (fixed and known) physical parameter τ . The left and right plots of Figure 2 depict $\max|\zeta|$ using $h_\tau = 0.01$ (note the difference in axes). We see that the maximum dissipation error decreases by an order of magnitude (to 0.02). We also note that, as seen in the right plot, the methods of different orders are virtually indistinguishable at this discretization level.

A similar result is observed in the plots of Figure 3 using $h_\tau = 0.001$ where the maximum dissipation error again decreases by an order of magnitude (to 0.002). It is interesting to note that the minimizer of the curves moves to the left by an order of magnitude as h_τ is likewise decreased, the minimum of the curve is approximately $1 - 2h_\tau$, and for larger wave numbers the curves converge slowly to $1 - h_\tau$.

6.2 Stability Analysis for Lorentz Media

6.2.1 $(2, 2M)$ KF schemes

We consider the $(2, 2M)$ scheme for discretizing Maxwell's equations coupled with the Lorentz polarization model presented in the form of equations (5.2a), (5.2b) along with equations

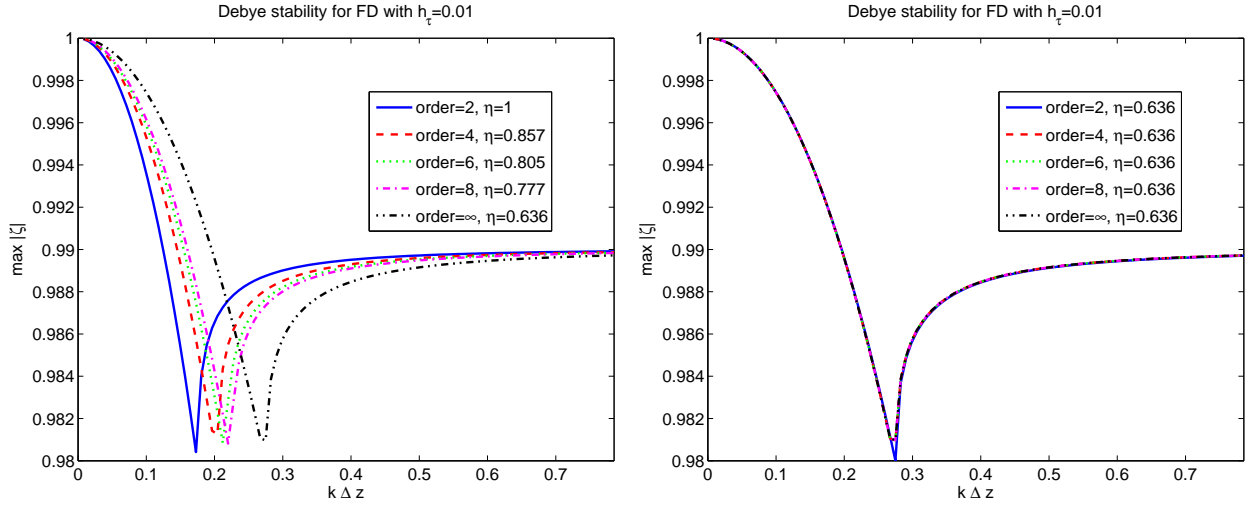


Figure 2: Left and right plots are similar to corresponding plots of Figure 1 except here $h_\tau = 0.01$. Note the change in axes from those of Figure 1.

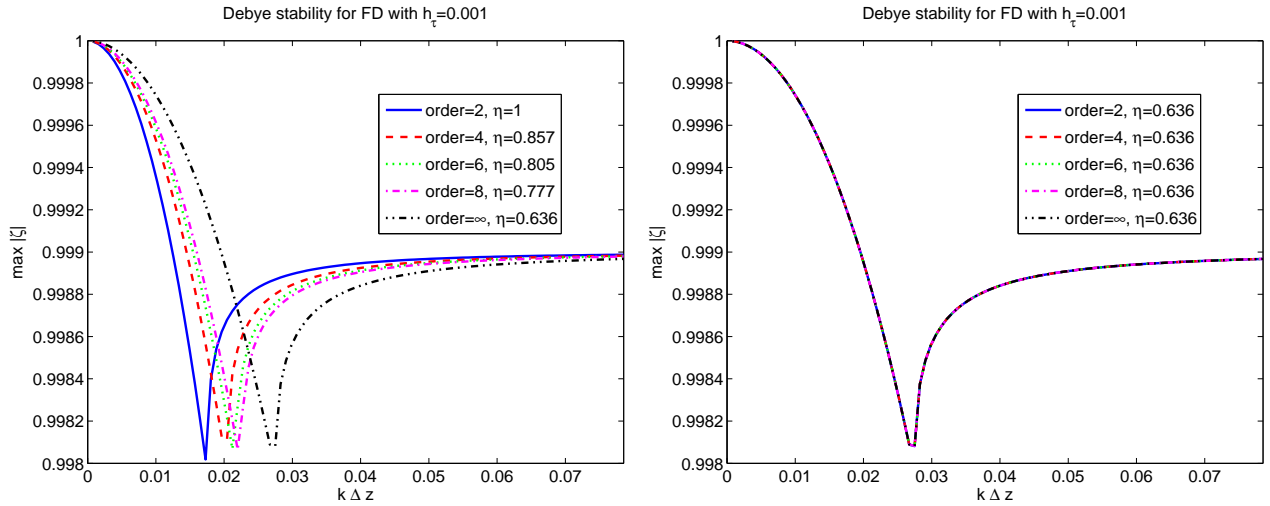


Figure 3: Left and right plot are similar to corresponding plots of Figure 1 except here $h_\tau = 0.001$. Note the change in axes from those of Figure 1.

(5.7) and (5.8). We rewrite the scheme using the (modified) variables $c_\infty B_{j+\frac{1}{2}}^{n-\frac{1}{2}}$, E_j^n , $\frac{1}{\epsilon_0 \epsilon_\infty} P_j^n$,

and $\frac{\Delta t}{\epsilon_0 \epsilon_\infty} J_j^n$ to get the modified system

(2, 2M)-KF:

$$c_\infty B_{j+\frac{1}{2}}^{n+\frac{1}{2}} = c_\infty B_{j+\frac{1}{2}}^{n-\frac{1}{2}} + \eta_\infty \sum_{p=1}^M \frac{\lambda_{2p-1}^{2M}}{2p-1} (E_{j+p}^n - E_{j-p+1}^n), \quad (6.16a)$$

$$E_j^{n+1} = E_j^n + \eta_\infty c_\infty \sum_{p=1}^M \frac{\lambda_{2p-1}^{2M}}{2p-1} (B_{j+p-\frac{1}{2}}^{n+\frac{1}{2}} - B_{j-p+\frac{1}{2}}^{n+\frac{1}{2}}) - \frac{1}{\epsilon_0 \epsilon_\infty} (P_j^{n+1} - P_j^n), \quad (6.16b)$$

$$P_j^{n+1} = P_j^n + \frac{\Delta t}{2} (J_j^{n+1} + J_j^n), \quad (6.16c)$$

$$J_j^{n+1} = J_j^n - \frac{\nu \Delta t}{2} (J_j^{n+1} - J_j^n) + \frac{\omega_p^2 \Delta t \epsilon_0}{2} (E_j^{n+1} - E_j^n) - \frac{\omega_0^2 \Delta t}{2} (P_j^{n+1} + P_j^n). \quad (6.16d)$$

As done for Debye media, we look for plane wave solutions of (6.16a)-(6.16d) as numerically evaluated at the discrete space-time points (t^n, x_j) or $(t^{n+1/2}, z_{j+1/2})$. We assume a spatial dependence of the form

$$B_{j+\frac{1}{2}}^{n+\frac{1}{2}} = \hat{B}^{n+\frac{1}{2}}(k) e^{ikz_{j+\frac{1}{2}}}, \quad (6.17a)$$

$$E_j^n = \hat{E}^n(k) e^{ikz_j}, \quad (6.17b)$$

$$P_j^n = \hat{P}^n(k) e^{ikz_j}, \quad (6.17c)$$

$$J_j^n = \hat{J}^n(k) e^{ikz_j}. \quad (6.17d)$$

where k is the wavenumber. The amplification matrix for this method is given by

$$\begin{bmatrix} 1 & -\sigma & 0 & 0 \\ \left(1 - \frac{\pi^2 h_0^2 (\eta_s - 1)}{\theta_+}\right) \sigma^* & (1-q) - \frac{(2-q)(\eta_s - 1)\pi^2 h_0^2}{\theta_+} & \frac{2\pi^2 h_0^2}{\theta_+} & \frac{-1}{\theta_+} \\ \frac{\pi^2 h_0^2 (\eta_s - 1)}{\theta_+} \sigma^* & \frac{(2-q)(\eta_s - 1)\pi^2 h_0^2}{\theta_+} & 1 - \frac{2\pi^2 h_0^2}{\theta_+} & \frac{1}{\theta_+} \\ \frac{2\pi^2 h_0^2 (\eta_s - 1)}{\theta_+} \sigma^* & \frac{2(2-q)(\eta_s - 1)\pi^2 h_0^2}{\theta_+} & \frac{-4\pi^2 h_0^2}{\theta_+} & \frac{2 - \theta_+}{\theta_+} \end{bmatrix}, \quad (6.18)$$

where the parameters h_0 and θ_+ are defined as

$$h_0 := \Delta t / T = (w_0 \Delta t) / (2\pi), \quad (6.19)$$

$$\theta_+ := 1 + h_\tau / 2 + \pi^2 h_0^2 \eta_s, \quad (6.20)$$

and the parameters σ and q are as given in (6.8) and (6.9), respectively. The parameters η_s and h_τ are defined in (6.5) and (6.4), respectively.

As in case of a Debye material, the characteristic polynomial retains the same structure as in [31] except for the inclusion of the parameter q .

$$P_{(2,2m)\text{-KF-L}}(X) = X^4 + X^3 \left(\frac{\theta_3 q + \theta'_3}{\theta_0} \right) + X^2 \left(\frac{\theta_2 q + \theta'_2}{\theta_0} \right) + X \left(\frac{\theta_1 q + \theta'_1}{\theta_0} \right) + \frac{\theta'_0}{\theta_0}, \quad (6.21)$$

where, the coefficients in (6.21) are defined as

$$\theta_3 = 2 + h_\tau + 2\pi^2 h_0^2, \quad (6.22)$$

$$\theta'_3 = -8 - 2h_\tau, \quad (6.23)$$

$$\theta_2 = 4\pi^2 h_0^2 - 4, \quad (6.24)$$

$$\theta'_2 = -4\pi^2 h_0^2 \eta_s + 12, \quad (6.25)$$

$$\theta_1 = 2 + 2\pi^2 h_0^2 - h_\tau, \quad (6.26)$$

$$\theta'_1 = -8 + 2h_\tau, \quad (6.27)$$

$$\theta'_0 = 2 - h_\tau + 2\pi^2 h_0^2 \eta_s, \quad (6.28)$$

$$\theta_0 = 2 + h_\tau + 2\pi^2 h_0^2 \eta_s. \quad (6.29)$$

Again, assuming that $\epsilon_s > \epsilon_\infty$, i.e., $\eta_s > 1$, and $\nu > 0$, and applying the results of the von-Neumann analysis conducted in [10] gives us the stability condition: $q \in (0, 4)$ for all wavenumbers, k , i.e.,

$$4\eta_\infty^2 \left(\sum_{p=1}^M \gamma_{2p-1} \sin^{2p-1} \left(\frac{kh}{2} \right) \right)^2 < 4, \quad \forall k, \quad (6.30)$$

which implies that

$$\eta_\infty \left(\sum_{p=1}^M \gamma_{2p-1} \right) < 1 \iff \eta_\infty \left(\sum_{p=1}^M \frac{[(2p-3)!!]^2}{(2p-1)!} \right) < 1. \quad (6.31)$$

Thus, for different values of M we obtain the following stability conditions

$$M = 1, \quad \eta_\infty < 1 \iff \Delta t < \frac{\Delta z}{c_\infty}, \quad (6.32a)$$

$$M = 2, \quad \eta_\infty \left(1 + \frac{1}{6} \right) < 1 \iff \Delta t < \frac{6\Delta z}{7c_\infty}, \quad (6.32b)$$

$$M = 3, \quad \eta_\infty \left(1 + \frac{1}{6} + \frac{3}{40} \right) < 1 \iff \Delta t < \frac{120\Delta z}{149c_\infty}, \quad (6.32c)$$

⋮

$$M = M, \quad \eta_\infty \left(\sum_{p=1}^M \gamma_{2p-1} \right) < 1 \iff \Delta t < \frac{\Delta z}{\left(\sum_{p=1}^M \frac{[(2p-3)!!]^2}{(2p-1)!} \right) c_\infty}, \quad (6.32d)$$

$$M = \infty, \quad \eta_\infty \left(\frac{\pi}{2} \right) < 1 \iff \Delta t < \frac{2\Delta z}{\pi c_\infty}. \quad (6.32e)$$

Again, the positivity of the coefficients γ_{2p-1} gives that the constraint in (6.32e) guarantees stability for all orders M .

6.2.2 Dissipation Error for $(2, 2M)$ KF Schemes for Lorentz Media

In the left plot of Figure 4 we graph the absolute value of the largest root of (6.21), as a function of $k\Delta z$, using $h_0 = 0.1$ for the $(2, 2M)$ KF schemes of orders $M = 2, 4, 6, 8$, given in equations (6.16a)-(6.16d), and the limiting ($M = \infty$) case with η_∞ set to the maximum stable value for each order, as given in (6.32). In the right plot we fix η_∞ to the maximum stable value for the limiting (order = ∞) case (i.e., each method uses the same value of η_∞ and that value is the largest for which all methods are guaranteed stable). As in the

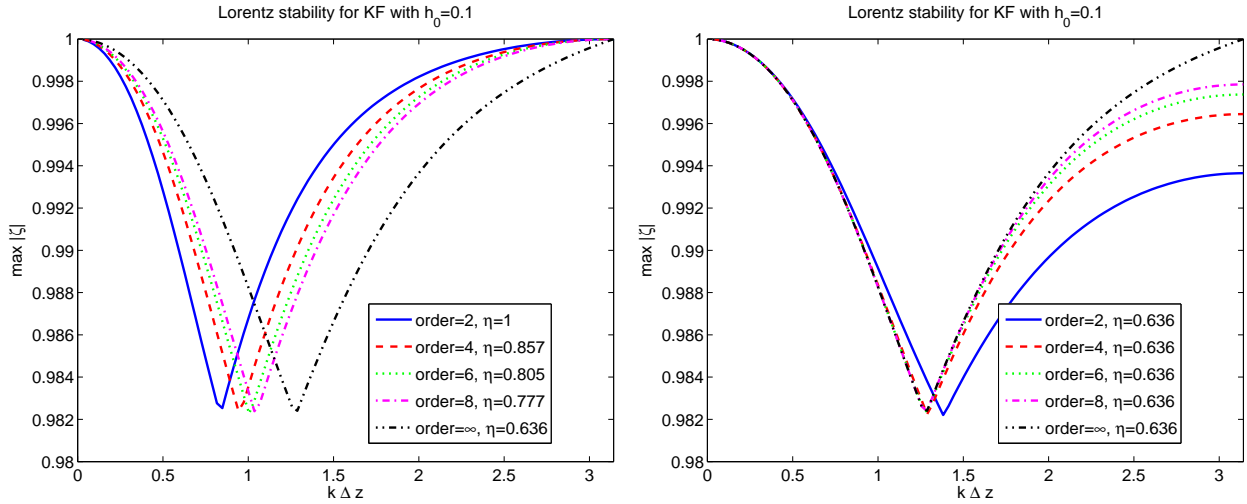


Figure 4: (Left) $\max|\zeta|$ versus $k\Delta z$ using $h_0 = 0.1$ for the $(2, 2M)$ KF schemes of orders $M = 2, 4, 6, 8$, given in equations (6.16a)-(6.16d), and the limiting ($M = \infty$) case with η_∞ set to the maximum stable value for the order, as given in (6.32). (Right) is with η_∞ fixed at the maximum stable value for the limiting ($M = \infty$) case.

Debye case, the left plot suggests that the infinite order method has the least dissipation for small values of $k\Delta z$, however this is mostly a consequence of the severe restriction on η_∞ . The right plot demonstrates that for all material and discretization parameters held fixed at equivalent values for all orders of the $(2, 2M)$ KF schemes, the second order method has the least dissipation for small $k\Delta z$, albeit only by a small amount. Refining the temporal discretization, as in the Debye analysis, we see that the methods of various orders conform, as depicted in Figures 5 and 6. It is interesting to note that the maximum dissipation error (defined here to be 1 minus the minimum value of the curve) for the $(2, 2M)$ KF schemes (and the assumed parameter values) is approximately $0.2h_0$, and the minimizer of the curves moves to the left by an order of magnitude as h_0 is likewise decreased. However, unlike in the Debye case, the dissipation error goes to zero as $k\Delta z$ increases, rather than converging to half of the maximum dissipation error. This is a promising result in the case of broad-band signals.

6.2.3 $(2, 2M)$ JHT schemes

Finally, we consider the $(2, 2M)$ schemes for discretizing Maxwell's equations coupled with the Lorentz polarization model presented in equations (5.2a), (5.2b) along with equation

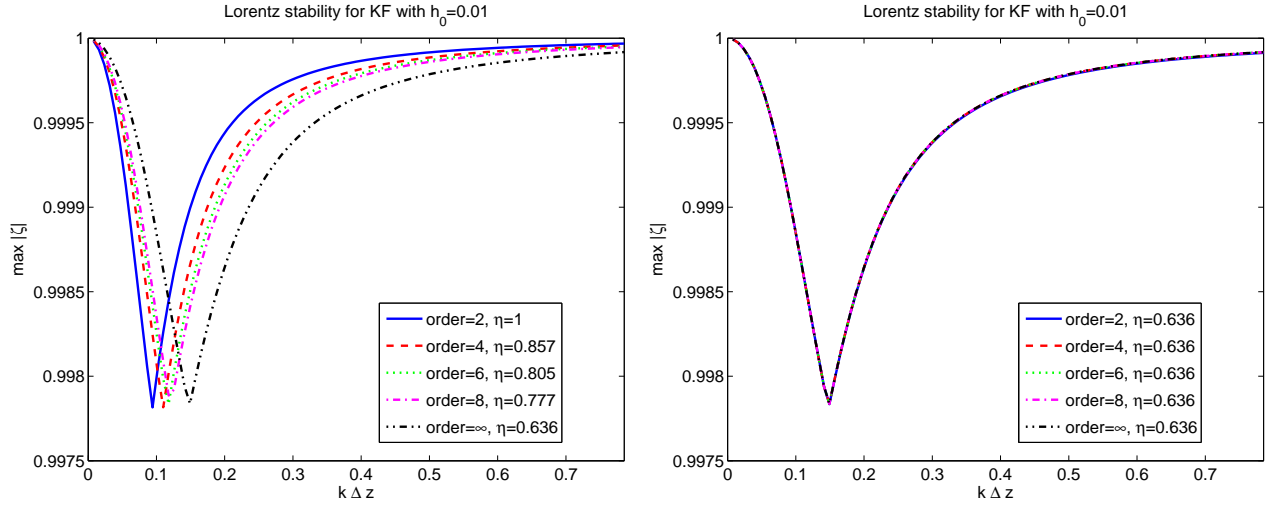


Figure 5: Left and right plots are similar to corresponding plots in Figure 4 except here $h_0 = 0.01$. Note the change in axes from the Figure 4.

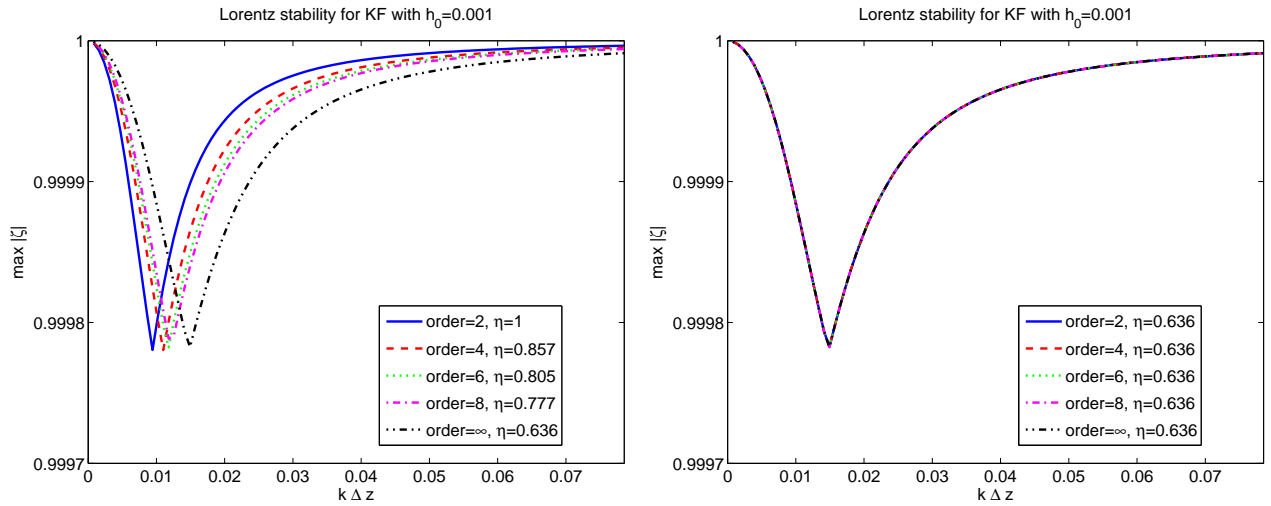


Figure 6: Left and right plots are similar to corresponding plots in Figure 4 except here $h_0 = 0.001$. Note the change in axes from the Figure 4.

(5.6). Using the (modified) variables $c_\infty B_{j+\frac{1}{2}}^{n-\frac{1}{2}}$, E_j^n , E_j^{n-1} , and $\frac{1}{\epsilon_0 \epsilon_\infty} D_j^n$ we rewrite this system

as

(2, 2M)-JHT:

$$c_\infty B_{j+\frac{1}{2}}^{n+\frac{1}{2}} = c_\infty B_{j+\frac{1}{2}}^{n-\frac{1}{2}} + \eta_\infty \sum_{p=1}^M \frac{\lambda_{2p-1}^{2M}}{2p-1} (E_{j+p}^n - E_{j-p+1}^n), \quad (6.33a)$$

$$\frac{1}{\epsilon_0 \epsilon_\infty} D_j^{n+1} = \frac{1}{\epsilon_0 \epsilon_\infty} D_j^n + \eta_\infty c_\infty \sum_{p=1}^M \frac{\lambda_{2p-1}^{2M}}{2p-1} (B_{j+p-\frac{1}{2}}^{n+\frac{1}{2}} - B_{j-p+\frac{1}{2}}^{n+\frac{1}{2}}), \quad (6.33b)$$

$$\begin{aligned} \frac{\phi_+}{2} E_j^{n+1} &= 2E_j^n - \frac{\phi_-}{2} E_j^{n-1} + \frac{1}{\epsilon_0 \epsilon_\infty} (D_j^{n+1} - 2D_j^n + D_j^{n-1}), \\ &+ \frac{h_\tau}{2} \frac{1}{\epsilon_0 \epsilon_\infty} (D_j^{n+1} - D_j^{n-1}) + 2\pi^2 h_0^2 \frac{1}{\epsilon_0 \epsilon_\infty} (D_j^{n+1} + D_j^{n-1}), \end{aligned} \quad (6.33c)$$

where the parameters ϕ_+ and ϕ_- are defined as

$$\phi_- := 2 - h_\tau + 4\pi^2 h_0^2 \eta_s, \quad (6.34)$$

$$\phi_+ := 2 + h_\tau + 4\pi^2 h_0^2 \eta_s, \quad (6.35)$$

with the parameters η_s and h_τ defined in (6.5) and (6.4), respectively, and the parameter h_0 as defined in (6.19).

We look for plane wave solutions of (6.33a)-(6.33c) as numerically evaluated at the discrete space-time points (t^n, x_j) or $(t^{n+1/2}, z_{j+1/2})$

$$B_{j+\frac{1}{2}}^{n+\frac{1}{2}} = \hat{B}^{n+\frac{1}{2}}(k) e^{ikz_{j+\frac{1}{2}}}, \quad (6.36)$$

$$E_j^n = \hat{E}^n(k) e^{ikz_j}, \quad (6.37)$$

$$D_j^n = \hat{D}^n(k) e^{ikz_j}. \quad (6.38)$$

The amplification matrix for this method is given by

$$\begin{bmatrix} 1 & -\sigma & 0 & 0 \\ \frac{\sigma^* h_\tau}{\phi_+} & \frac{2 - q(1 + h_\tau/2 + 2\pi^2 h_0^2)}{\phi_+} & \frac{-\phi_-}{\phi_+} & \frac{4\pi^2 h_0^2}{\phi_+} \\ 0 & 1 & 0 & 0 \\ \sigma^* & -q & 0 & 1 \end{bmatrix}, \quad (6.39)$$

where σ and q are as defined in (6.8) and (6.9), respectively.

The characteristic polynomial for the JHT scheme for the Lorentz model becomes

$$P_{(2,2m)\text{-JHT-L}}(X) = X^4 + X^3 \left(\frac{\phi_3 q + \phi'_3}{\phi_+} \right) + X^2 \left(\frac{\phi_2 q + \phi'_2}{\phi_+} \right) + X \left(\frac{\phi_1 q + \phi'_1}{\phi_+} \right) + \frac{\phi_-}{\phi_+}, \quad (6.40)$$

where, the coefficients are given to be:

$$\phi_3 := 2 + h_\tau + 4\pi^2 h_0^2, \quad (6.41)$$

$$\phi'_3 := -8 - 2h_\tau - 8\pi^2 h_0^2 \eta_s, \quad (6.42)$$

$$\phi_2 := -4, \quad (6.43)$$

$$\phi'_2 := 8\pi^2 h_0^2 \eta_s + 12, \quad (6.44)$$

$$\phi_1 := 2 + 4\pi^2 h_0^2 - h_\tau, \quad (6.45)$$

$$\phi'_1 := -8 - 2h_\tau - 8\pi^2 h_0^2 \eta_s. \quad (6.46)$$

Again, we are able to retain the same structure for the characteristic polynomial as in [31] except for the inclusion of the parameter q , and it is equivalent to the characteristic polynomial in [10].

Again, assuming that $\epsilon_s > \epsilon_\infty$, i.e., $\eta_s > 1$, and $\nu > 0$, and applying the results of the von-Neumann analysis conducted in [10] gives us the following stability condition: $q \in (0, 2)$, for all wavenumbers, k i.e.,

$$4\eta_\infty^2 \left(\sum_{p=1}^M \gamma_{2p-1} \sin^{2p-1} \left(\frac{kh}{2} \right) \right)^2 < 2, \quad \forall k, \quad (6.47)$$

which implies that

$$\eta_\infty \left(\sum_{p=1}^M \gamma_{2p-1} \right) < \frac{1}{\sqrt{2}} \iff \eta_\infty \left(\sum_{p=1}^M \frac{[(2p-3)!!]^2}{(2p-1)!} \right) < \frac{1}{\sqrt{2}}. \quad (6.48)$$

Thus, for different values of M we obtain the following stability conditions

$$M = 1, \quad \eta_\infty < \frac{1}{\sqrt{2}} \iff \Delta t < \frac{\Delta z}{\sqrt{2}c_\infty}, \quad (6.49a)$$

$$M = 2, \quad \eta_\infty \left(1 + \frac{1}{6} \right) < \frac{1}{\sqrt{2}} \iff \Delta t < \frac{6\Delta z}{7\sqrt{2}c_\infty}, \quad (6.49b)$$

$$M = 3, \quad \eta_\infty \left(1 + \frac{1}{6} + \frac{3}{40} \right) < \frac{1}{\sqrt{2}} \iff \Delta t < \frac{120\Delta z}{149\sqrt{2}c_\infty}, \quad (6.49c)$$

$$\vdots \quad (6.49d)$$

$$M = M, \quad \eta_\infty \left(\sum_{p=1}^M \gamma_{2p-1} \right) < \frac{1}{\sqrt{2}} \iff \Delta t < \frac{\Delta z}{\left(\sum_{p=1}^M \frac{[(2p-3)!!]^2}{(2p-1)!} \right) \sqrt{2}c_\infty}, \quad (6.49e)$$

$$M = \infty, \quad \eta_\infty \left(\frac{\pi}{2} \right) < \frac{1}{\sqrt{2}} \iff \Delta t < \frac{\sqrt{2}\Delta z}{\pi c_\infty}. \quad (6.49f)$$

Again, the positivity of the coefficients γ_{2p-1} gives that the constraint in (6.49f) guarantees stability for all orders M .

6.2.4 Dissipation Error for $(2, 2M)$ JHT Schemes for Lorentz Media

As before, in the left plot of Figure 7 we graph the absolute value of the largest root of (6.40), as a function of $k\Delta z$, using $h_0 = 0.1$ for the $(2, 2M)$ JHT schemes of orders $M = 2, 4, 6, 8$, given in equations (6.33a)-(6.33c), and the limiting ($M = \infty$) case with η_∞ set to the maximum stable value for each order, as given in (6.49). Again, in the right plot we fix η_∞ to the maximum stable value for the limiting ($M = \infty$) case. While numerically different,

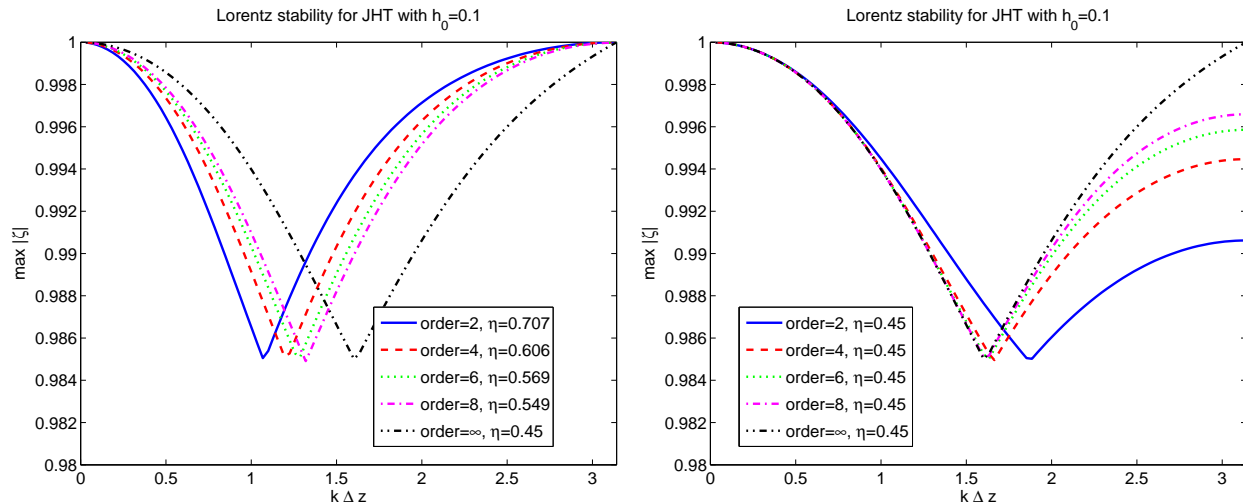


Figure 7: (Left) $\max|\zeta|$ versus $k\Delta z$ using $h_0 = 0.1$ for the $(2, 2M)$ JHT schemes of orders $M = 2, 4, 6, 8$, given in equations (6.33a)-(6.33c), and the limiting ($M = \infty$) case with η_∞ set to the maximum stable value for the order, as given in (6.49). (Right) η_∞ fixed at the maximum stable value for the limiting ($M = \infty$) case.

the dissipation plots for the $(2, 2M)$ JHT schemes with $h_0 = 0.1$ are qualitatively the same as those for the KF scheme. Figures 8 and 9 contain plots using $h_0 = 0.01$ and $h_0 = 0.001$, respectively (again, note the change in axes). Although the stability condition for $(2, 2M)$ JHT schemes are more restrictive, there is no distinct advantage over the (corresponding) $(2, 2M)$ KF schemes with respect to dissipation error resulting from enforcing this constraint. The magnitude of the dissipation errors, while slightly less for fixed values of $k\Delta z$, seem to be comparable to those of the (corresponding) $(2, 2M)$ KF schemes. As in the Debye analysis, the effect of the order of the method is negligible when considering small discretization parameters (whether h_0 or $k\Delta z$) and holding the value of η_∞ fixed.

7 Dispersion Analysis

A time dependent scalar linear partial differential equation (PDE) with constant coefficients on an unbounded space domain admits plane wave solutions of the form $e^{i(kz-\omega t)}$, where k is the wave number and ω the frequency. The PDE imposes a relation of the form $\omega = \omega(k)$, which is called a dispersion relation. The PDE itself is called dispersive if the speed of propagation of waves depends on the wave number k (or on ω). Finite difference approximations on uniform meshes to the PDEs also admit plane wave solutions. Regardless of whether the

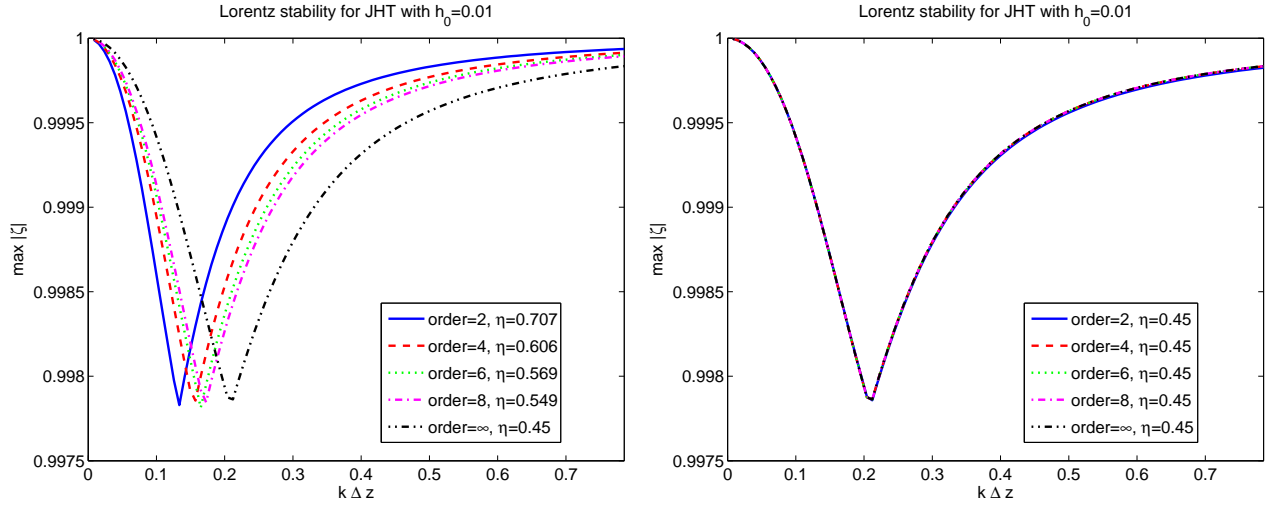


Figure 8: Left and right plot are similar to Figure 7 except here $h_0 = 0.01$. Note the change in axes from that of Figure 7.

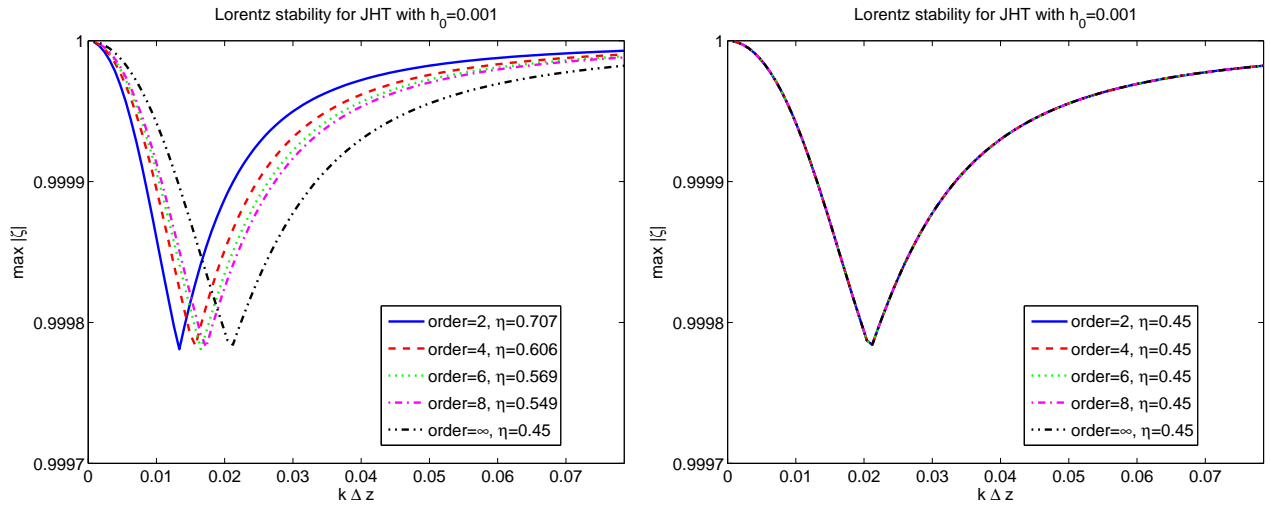


Figure 9: Left and right plot are similar to Figure 7 except here $h_0 = 0.001$. Note the change in axes from that of Figure 7.

PDE is dispersive, any finite difference approximation will exhibit spurious dispersion [41]. The dispersion relation of the numerical method is called a numerical dispersion relation as it is an artifact of the numerical scheme.

As mentioned in the introduction, the models for Debye and Lorentz media have actual physical dispersion which needs to be modeled correctly. In this section we construct the numerical dispersion relations for the $(2, 2M)$ schemes considered in Section 5 for Debye and Lorentz dispersive media. We plot the phase error for all these different methods by using representative values for all the parameters of each model. We follow the approach in [31] in which dispersion analysis was conducted for the $(2, 2)$ (or Yee) finite difference scheme for Debye and Lorentz media.

7.1 Debye Media

A plane wave solution of the continuous Debye model 1, given in equations (2.7a) and (2.7b) which are appended to the Maxwell system (3.2a) and (3.2b), gives us the following (exact) dispersion relation

$$k_{\text{EX}}^{\text{D}}(\omega) = \frac{\omega}{c} \sqrt{\epsilon_r^{\text{D}}(\omega)}. \quad (7.1)$$

where

$$\epsilon_r^{\text{D}}(\omega) := \frac{\epsilon_s \lambda - i\omega \epsilon_\infty}{\lambda - i\omega}, \quad (7.2)$$

is the relative complex permittivity of the Debye medium, $\lambda = 1/\tau$ and ω is the angular frequency.

We consider the $(2, 2M)$ th order finite difference schemes for Debye media given in (6.1a), (6.1b) and (6.1c) and similarly consider plane wave solutions of this discrete system. We define the quantity

$$K_{\text{FD}}^{\text{D}}(\omega) := \frac{2}{\Delta z} \sum_{p=1}^M \gamma_{2p-1} \sin^{2p-1} \left(\frac{k_{\text{FD}}^{\text{D}}(\omega) \Delta z}{2} \right), \quad (7.3)$$

where k_{FD}^{D} is the numerical wave number. We solve for k_{FD}^{D} from the numerical dispersion relation for this scheme which can be computed by assuming a plane wave solution of the form $e^{i(k_{\text{FD}}^{\text{D}} z - \omega t)}$ for all the discrete variables in the $(2, 2M)$ Debye finite difference methods (6.1a), (6.1b) and (6.1c) and is given as

$$K_{\text{FD}}^{\text{D}}(\omega) = \frac{\omega \Delta}{c} \sqrt{\epsilon_{r,\text{FD}}^{\text{D}}}, \quad (7.4)$$

where

$$\epsilon_{r,\text{FD}}^{\text{D}} := \frac{\epsilon_{s,\Delta} \lambda_\Delta - i\omega_\Delta \epsilon_{\infty,\Delta}}{\lambda_\Delta - i\omega_\Delta}. \quad (7.5)$$

This notation corresponds to the following discrete representations of the continuous model parameters:

$$\epsilon_{s,\Delta} := \epsilon_s, \quad (7.6a)$$

$$\epsilon_{\infty,\Delta} := \epsilon_\infty, \quad (7.6b)$$

$$\lambda_\Delta := \lambda \cos(\omega \Delta t / 2), \quad (7.6c)$$

and a representation of the frequency by

$$\omega_\Delta := \omega \frac{\sin(\omega \Delta t / 2)}{(\omega \Delta t) / 2}. \quad (7.7)$$

We define the phase error Φ as

$$\Phi = \left| \frac{k_{\text{EX}} - k_{\text{FD}}}{k_{\text{EX}}} \right|. \quad (7.8)$$

We wish to examine the phase error as a function of $\omega\Delta t$ in the range $[0, \pi]$. We note that $\omega\Delta t = 2\pi/N_{\text{ppp}}$, where N_{ppp} is the number of points per period, and is related to the number of points per wavelength (N_{ppw}) via

$$N_{\text{ppw}} = \eta_{\infty} N_{\text{ppp}}. \quad (7.9)$$

Thus, for $\eta_{\infty} \leq 1$, the number of points per wavelength is always less than or equal to the number of points per period. Note that the number of points per wavelength in the range $[\pi/4, \pi]$ is 8 to 2 points per period. We are more interested in the range $[0, \pi/4]$ which involves more than 8 points per period.

To generate the plots below we have used the following values for the medium parameters as :

$$\epsilon_{\infty} = 1, \quad (7.10)$$

$$\epsilon_s = 78.2, \quad (7.11)$$

$$\tau = 8.1 \times 10^{-12} \text{ sec}. \quad (7.12)$$

In the plots of Figure 10 we depict graphs of the phase error ϕ defined in (7.8), versus $\omega\Delta t$, for the $(2, 2M)$ th order finite difference methods applied to the Debye model, as given in equations (6.1a)-(6.1c), for orders 2, 4, 6, 8 and the limiting ($M = \infty$) case. The temporal refinement factor, $h_{\tau} = \Delta t/\tau$, is fixed at 0.1. The left plot uses values of η_{∞} set to the maximum stable value for the order, as given in (6.13), while the right plot fixes η_{∞} at the maximum stable value for the limiting ($M = \infty$) case as given in (6.14) (i.e., the maximum stable value for all orders).

In both plots it appears as though the infinite order method has the least dispersion error over a vast majority of the domain. However, looking at the intermediate orders, it is clear that at some value of $\omega\Delta t$ each higher order method begins to have more dispersion than the next lower order method for increasing values of $\omega\Delta t$. Generally speaking, the higher order methods reward large N_{ppp} more than lower order methods do, but penalize low N_{ppp} . The right plot demonstrates that fixing the value of η_{∞} to be constant across orders of methods tends to exaggerate this behavior.

Figures 11 and 12 depict similar plots as in Figure 10, except with $h_{\tau} = 0.01$ and 0.001 , respectively. Comparing the left plots, there does not appear to be much improvement in any of the higher order methods with respect to dispersion error. Only the second order method seems to benefit. In fact, the plots suggest that the second order method is vastly superior to the higher order methods. Contrast this with the stability plots in Figures 2 and 3 which showed orders of magnitude decreases in error for all orders with corresponding decreases in discretization parameters. However, note that decreasing h_{τ} changes Δt , thus to compare Φ at consistent values of $\omega\Delta t$ we should be looking at different intervals in these plots. It is more straight-forward to compare various h_{τ} values on a plot of Φ versus only ω , as shown in Figures 13-15 below. There we can clearly see orders of magnitude decreases in Φ as h_{τ} is decreased. In fact, now it is apparent that for the frequencies of interest (i.e., those near $\omega\tau = 1$), the higher order methods exhibit a gradual improvement over the second order method.

Comparing left plots of Figures 10-12 with the right plots, the effect of using a small Δt is that the error associated with choosing an η_{∞} much smaller than the maximum stable

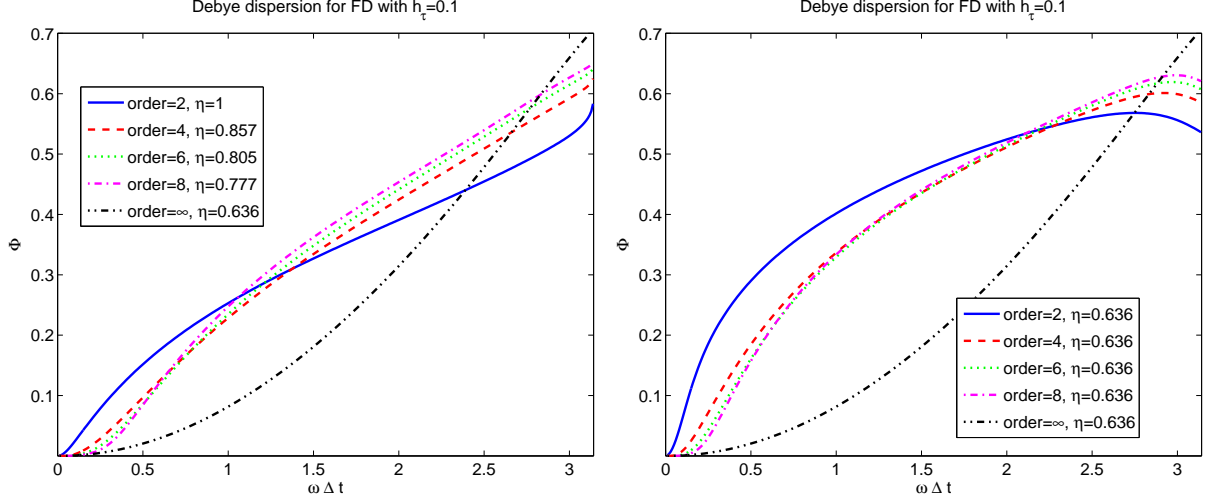


Figure 10: (Left) Phase error ϕ versus $\omega\Delta t$ using $h_\tau = 0.1$ for the finite difference schemes for the Debye model, given in (6.1a)-(6.1c), of orders 2, 4, 6, 8 and the limiting ($M = \infty$) case with η_∞ set to the maximum stable value for the order, as given in (6.13). (Right) The parameter η_∞ is fixed at the maximum stable value for the limiting ($M = \infty$) case, as given in (6.14).

value gets magnified. In fact, it appears as though the error for the second order method using $\eta_\infty = 0.636$ is larger with a smaller Δt ! However, again, Δt is changing from one plot to another, so the correct interpretation is that using a small Δt penalizes large N_{ppp} more so than using a larger Δt would. Looking at the left plots versus the right plots of Figures 14-15 there is almost no difference.

Lastly, we observe that decreasing the discretization parameter Δt results in a converging of the methods of various orders, with the notable exception of the second order method. While Figure 12 seemed to suggest that the second order method was vastly superior for fine discretizations, Figure 15 contradicts that assumption utterly.

7.2 Lorentz Media

The dispersion relation for the continuous Lorentz model is given by

$$k_{\text{EX}}^{\text{L}}(\omega) = \frac{\omega}{c} \sqrt{\epsilon_r^{\text{L}}(\omega)}. \quad (7.13)$$

where the relative complex permittivity for Lorentz media is given to be

$$\epsilon_r^{\text{L}}(\omega) := \frac{\omega^2 \epsilon_\infty - \epsilon_s \omega_0^2 + i\lambda \omega \epsilon_\infty}{\omega^2 - \omega_0^2 + i\lambda \omega}. \quad (7.14)$$

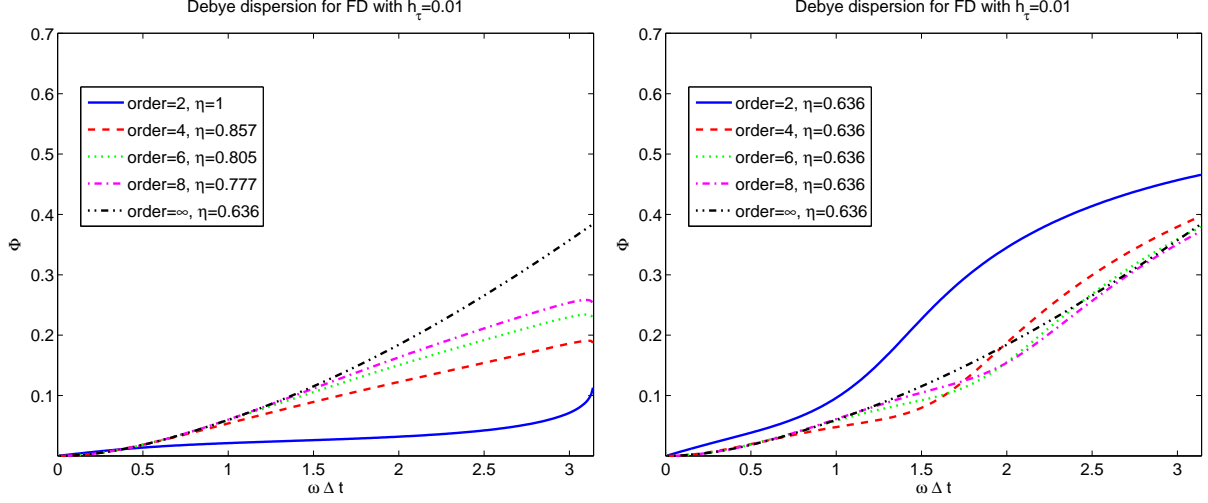


Figure 11: Left and right plots are similar to corresponding plots in Figure 10 except here $h_\tau = 0.01$.

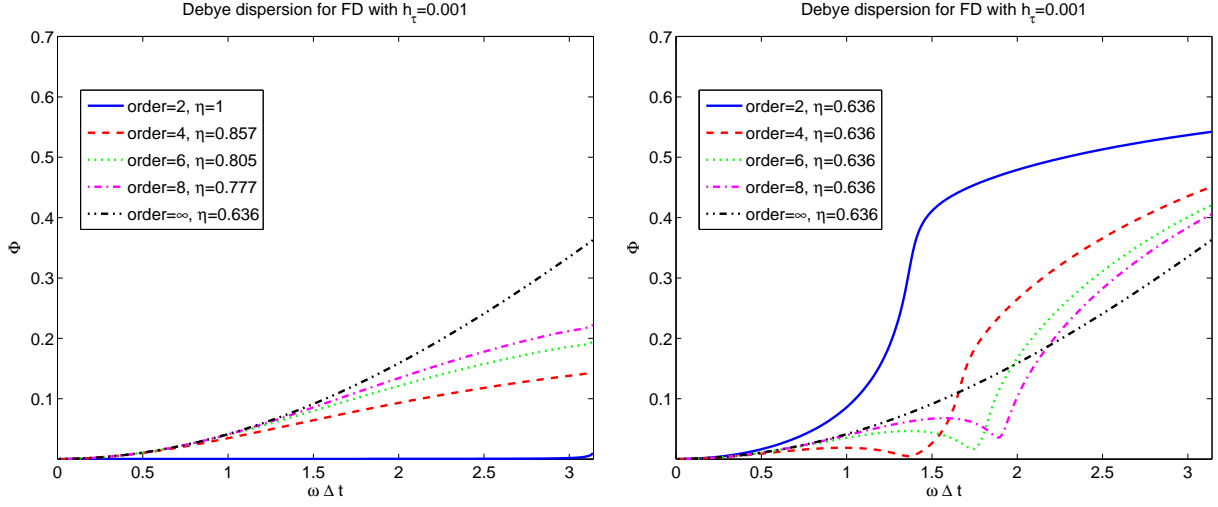


Figure 12: Left and right plots are similar to corresponding plots in Figure 10 except here $h_\tau = 0.001$.

7.2.1 $(2, 2M)$ KF Schemes

We consider the $(2, 2M)$ KF schemes for Lorentz media presented in equations (6.16a)-(6.16d). We define the quantity

$$K_{\text{KF},M}^L(\omega) := \frac{2}{\Delta z} \sum_{p=1}^M \gamma_{2p-1} \sin^{2p-1} \left(\frac{k_{\text{KF},M}^L(\omega) \Delta z}{2} \right), \quad (7.15)$$

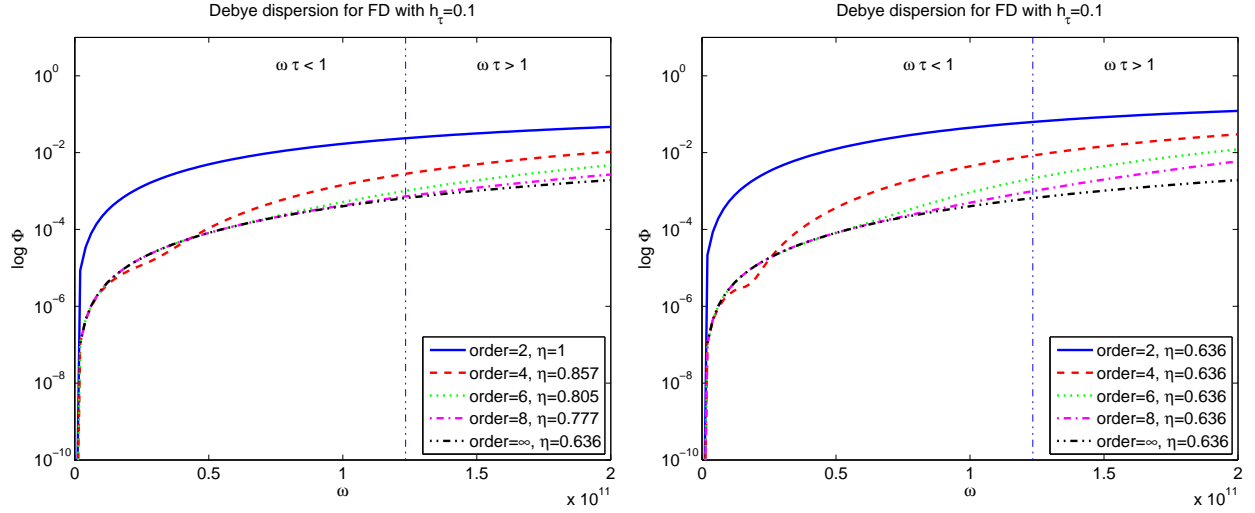


Figure 13: Plot on left is a log plot of the phase error ϕ versus ω using $h_\tau = 0.1$ for the FD scheme for the Debye model of orders 2, 4, 6, 8 and the limiting (order = ∞) case with η set to the maximum stable value for the order. Vertical line distinguishes region of $\omega\tau < 1$ from $\omega\tau > 1$. Plot on right is with η fixed at the maximum stable value for the limiting (order = ∞) case.

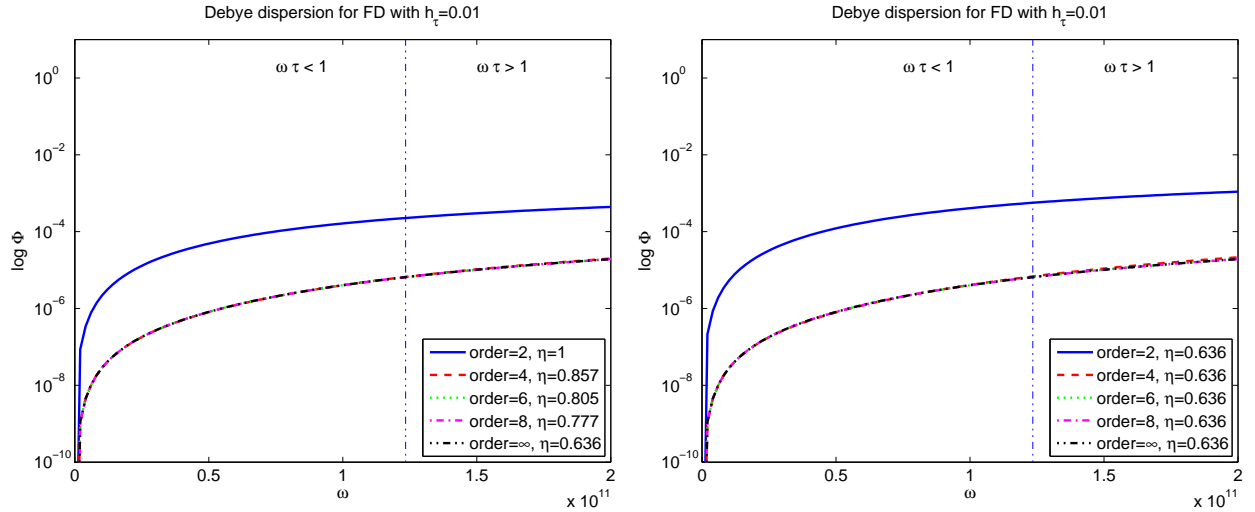


Figure 14: Left and right plot are similar to previous figure except here using $h_\tau = 0.01$.

where $k_{\text{KF},M}^L$ is the numerical wave number. We solve for $k_{\text{KF},M}^L$ from the dispersion relation for this scheme which can be computed as

$$K_{\text{KF}}^L(\omega) = \frac{\omega\Delta}{c} \sqrt{\epsilon_{r,\text{KF}}^L}, \quad (7.16)$$

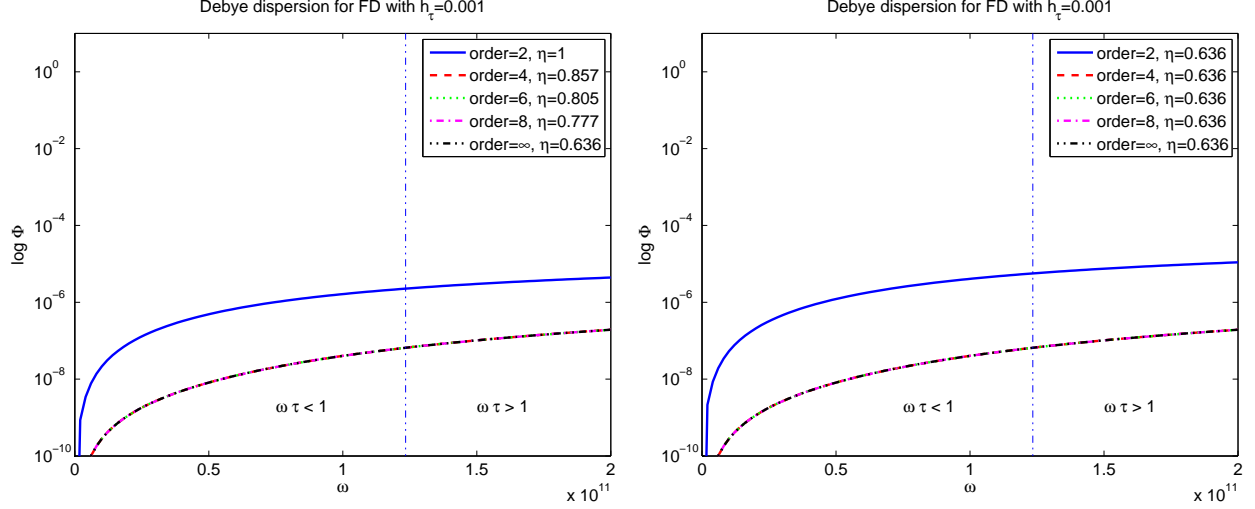


Figure 15: Left and right plot are similar to previous figure except here using $h_\tau = 0.001$.

where the discrete relative complex permittivity for the $(2, 2M)$ KF schemes is

$$\epsilon_{r,KF}^L := \frac{\omega_\Delta^2 \epsilon_{\infty,\Delta} - \epsilon_{s,\Delta} \tilde{\omega}_{0,\Delta}^2 + i\lambda_\Delta \omega_\Delta \epsilon_{\infty,\Delta}}{\omega_\Delta^2 - \tilde{\omega}_{0,\Delta}^2 + i\lambda_\Delta \omega_\Delta}, \quad (7.17)$$

with the discrete representations of the continuous model parameters as defined in (7.6) and (7.7), as well as

$$\tilde{\omega}_{0,\Delta} := \omega_0 \cos(\omega \Delta t / 2). \quad (7.18)$$

7.2.2 $(2, 2M)$ JHT schemes

We consider the $(2, 2M)$ JHT schemes for Lorentz media presented in equations (6.33a)-(6.33c) We define the quantity

$$K_{\text{JHT},M}^L(\omega) := \frac{2}{\Delta z} \sum_{p=1}^M \gamma_{2p-1} \sin^{2p-1} \left(\frac{k_{\text{JHT},M}^L(\omega) \Delta z}{2} \right), \quad (7.19)$$

where $k_{\text{JHT},M}^L$ is the numerical wave number. We solve for $k_{\text{JHT},M}^L$ from the dispersion relation for this scheme which is given as

$$K_{\text{JHT},M}^L(\omega) = \frac{\omega_\Delta}{c} \sqrt{\epsilon_{r,\text{JHT}}^L}, \quad (7.20)$$

where the discrete relative complex permittivity for the JHT scheme is

$$\epsilon_{r,\text{JHT}}^L := \frac{\omega_\Delta^2 \epsilon_{\infty,\Delta} - \epsilon_{s,\Delta} \omega_{0,\Delta}^2 + i\lambda_\Delta \omega_\Delta \epsilon_{\infty,\Delta}}{\omega_\Delta^2 - \omega_{0,\Delta}^2 + i\lambda_\Delta \omega_\Delta}, \quad (7.21)$$

with the discrete representations of the continuous model parameters as defined in (7.6) and (7.7) as well as

$$\omega_{0,\Delta} := \omega_0 \sqrt{\cos(\omega \Delta t)}. \quad (7.22)$$

7.2.3 Phase Error of KF and JHT schemes

In this section, we analyze plots of the phase error Φ for the $(2, 2M)$ th order KF and the JHT finite difference schemes applied to Lorentz media. The phase error is defined here as

$$\Phi := \left| \frac{k_{\text{EX}} - k_{\text{FD}}}{k_{\text{EX}}} \right|. \quad (7.23)$$

where now k_{EX} is given by (7.13) and k_{FD} is either $k_{\text{KF},M}^{\text{L}}$ or $k_{\text{JHT},M}^{\text{L}}$. The phase error is plotted against values of $\omega\Delta t$ in the range $[0, \pi]$.

To generate the plots below we have used the Lorentz model material parameters chosen by Brillouin [12], which are as follows:

$$\epsilon_{\infty} = 1, \quad (7.24)$$

$$\epsilon_s = 2.25, \quad (7.25)$$

$$\tau = 1.786 \times 10^{-16} \text{ sec}, \quad (7.26)$$

$$\omega_0 = 4 \times 10^{16} \text{ rad/sec}. \quad (7.27)$$

In the plots of Figure 16 we depict graphs of the phase error Φ defined in (7.23), versus $\omega\Delta t$, for the $(2, 2M)$ th order KF finite difference methods applied to the Lorentz model, given in equations (6.16a)-(6.16d), for orders 2, 4, 6, 8 and the limiting ($M = \infty$) case. The temporal refinement factor, $h_0 = \Delta t/\omega_0$, is fixed at 0.1. The left plot uses values of η_{∞} set to the maximum stable value for the order, while the right plot fixes η_{∞} at the maximum stable value for the limiting ($M = \infty$) case (i.e., the maximum stable value for all orders). These bounds for η_{∞} are given in (6.32).

The qualitative behavior of the curves is much different here than for the Debye model depicted in Figure 10, however, the basic result is the same. That is the infinite order method has the least dispersion for the vast majority of refinement values of interest, and in general at some value of $\omega\Delta t$ each higher order method begins to have more dispersion than the next lower order method for increasing values of $\omega\Delta t$. For the right plot of Figure 16 the behavior of the curves for high $\omega\Delta t$ is instead dominated by the restriction of η_{∞} . In particular, the second order method has very large dispersion for $\omega\Delta t > 1.5$. This result does not change as the temporal refinement, h_0 is decreased, as was the case for the Debye model (see the right plot in Figure 17 where $h_0 = 0.01$ and compare to Figure 12 for the Debye model).

The left plot in Figure 17 also was generated with $h_0 = 0.01$ and demonstrates that the dispersion for large $\omega\Delta t$ did not improve for the higher order methods. In fact, decreasing h_0 even further has no effect: the left and right plots of Figure 18 generated with $h_0 = 0.001$ are interesting in that there is almost no change from the previous case. Only the resonance peaks (e.g., corresponding to $\omega\Delta t = 1$ in Figure 16) are now too close to zero and too small to be seen. In particular, the left plot of Figure 18 suggests that the second order method with $\eta_{\infty} = 1$ is far superior to all other orders of methods for the $(2, 2M)$ KF schemes applied to the Lorentz polarization model.

In the plots of Figure 19 we depict graphs of the phase error Φ defined in (7.23), versus $\omega\Delta t$, for the $(2, 2M)$ th order JHT finite difference methods applied to the Lorentz model, given in equations (6.33a)-(6.33c), for orders 2, 4, 6, 8 and the limiting ($M = \infty$) case. Again, the temporal refinement factor, $h_0 = \Delta t/\omega_0$, is fixed at 0.1.

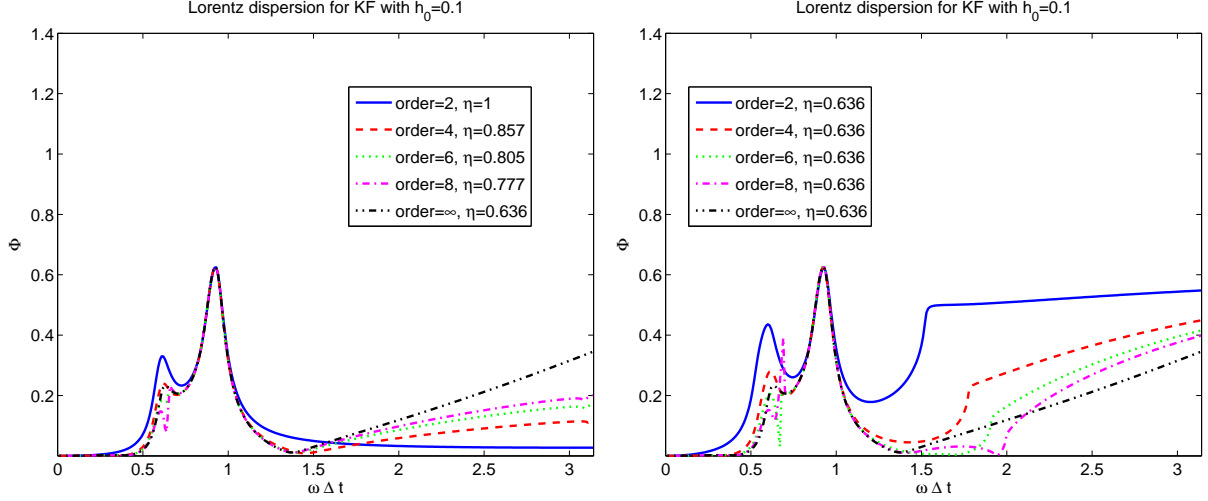


Figure 16: (Left) Phase error ϕ versus $\omega\Delta t$ using $h_0 = 0.1$ for the $(2, 2M)$ KF scheme for the Lorentz model, given in equations (6.16a)-(6.16d), of orders 2, 4, 6, 8 and the limiting ($M = \infty$) case with η_∞ set to the maximum stable value for the order. Plot on right is with η_∞ fixed at the maximum stable value for the limiting ($M = \infty$) case, where the bounds for η_∞ are given in (6.32).

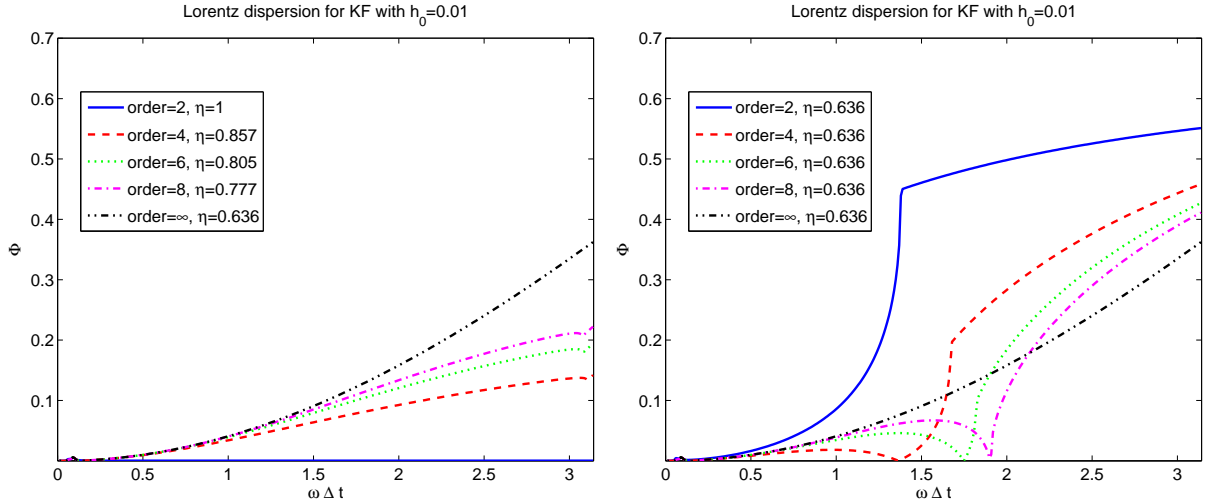


Figure 17: Left and right plots are similar to corresponding plots in Figure 16 except here $h_0 = 0.01$. Note the change in axes from that of Figure 16.

The qualitative behavior of the curves here is very similar to those of the corresponding $(2, 2M)$ KF schemes depicted in Figure 16, with the notable exception of the dispersion for large $\omega\Delta t$. For the $(2, 2M)$ JHT schemes, both the left and right plots exhibit the large dispersion errors for the lower order methods for $\omega\Delta t > 1.5$. This was noticed in [31] for the

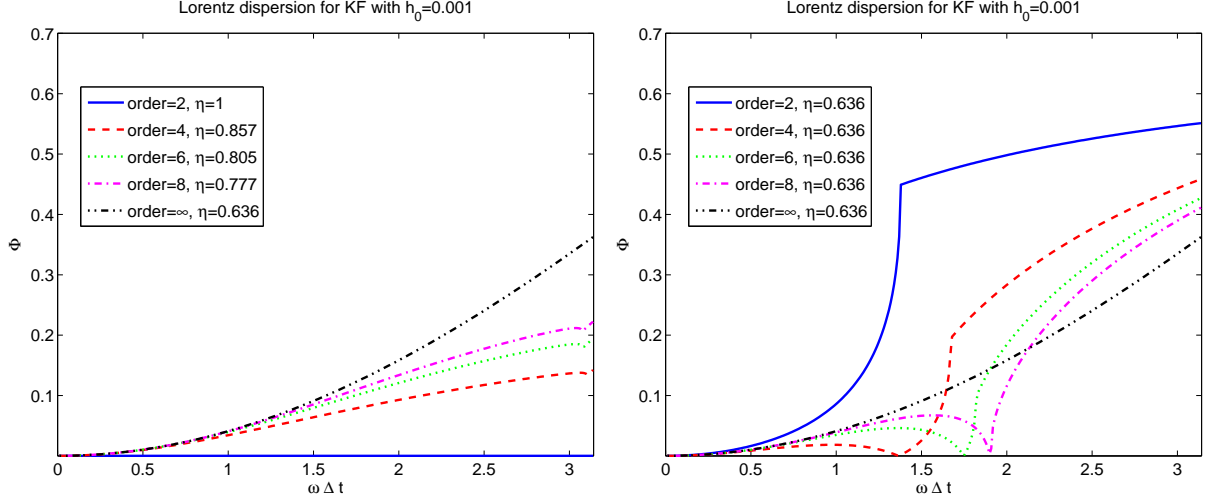


Figure 18: Left and right plots are similar to corresponding plots in Figure 16 except here $h_0 = 0.001$. Note the change in axes from that of Figure 16.

(2, 2) JHT scheme, and cited as a reason to prefer the (2, 2) KF scheme. Note that this is a direct result of the stability constraint on the (2, $2M$) JHT schemes in that $\eta_\infty < 1$ even for the second order method. Interestingly, there is no value of $\omega\Delta t$ at which each higher order method begins to have more dispersion than the next lower order method for increasing values of $\omega\Delta t$, as was the case for the Debye model and the KF scheme for Lorentz.

The dispersion curves in the right plots of Figures 20 and 21 have the same qualitative structure as those corresponding to the KF scheme, however here the left plots have similar properties due to the constraints on η_∞ .

It would appear from comparing all of the dispersion curves for KF and JHT schemes that the second order KF scheme is preferable for all temporal refinements $h_0 \leq 0.01$. However, again we note that decreasing h_τ changes Δt , thus to compare consistent quantities we should compare various h_τ values on a plot of Φ versus only ω , as shown in Figures 22-27 below. There we can clearly see orders of magnitude decreases in Φ for the frequencies of interest (i.e., those near $\omega/\omega_0 = 1$) as h_τ is decreased. Further, there is significantly less difference between the high frequency dispersion in the JHT scheme versus the KF scheme even for the second order method, than the $\omega\Delta t$ plots suggested. For instance, comparing the second order method in the left plot of Figure 24 or that of Figure 27 near $\omega = 8 \times 10^8$ Hz, there is less than an order of magnitude difference. (Arguably, the stability restriction still favors the KF scheme in terms of computational runtime.) Lastly, now it is apparent that each of the higher order methods exhibits a significant improvement over the second order method (for some frequencies, at least an order of magnitude), however, there is little accuracy gained by orders greater than 4 except for the very highest frequencies and for large values of h_0 .

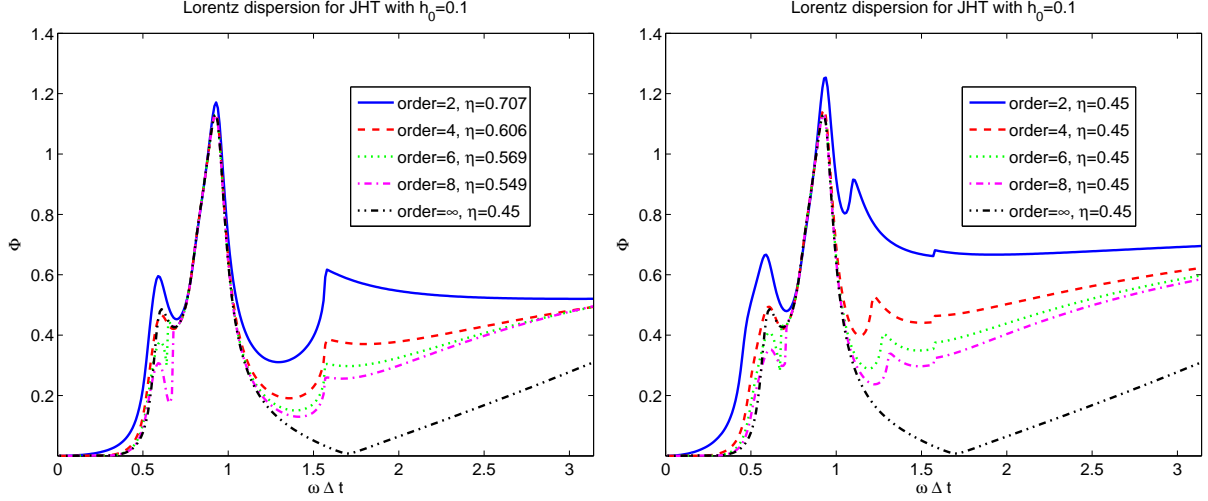


Figure 19: (Left) Phase error ϕ versus $\omega \Delta t$ using $h_0 = 0.1$ for the JHT scheme for the Lorentz model, given in equations (6.33a)-(6.33c), of orders 2, 4, 6, 8 and the limiting ($M = \infty$) case. The parameter η_∞ is set to the maximum stable value for the order, as given in (6.49). (Right) The parameter η_∞ fixed at the maximum stable value for the limiting ($M = \infty$) case, as given in (6.49).

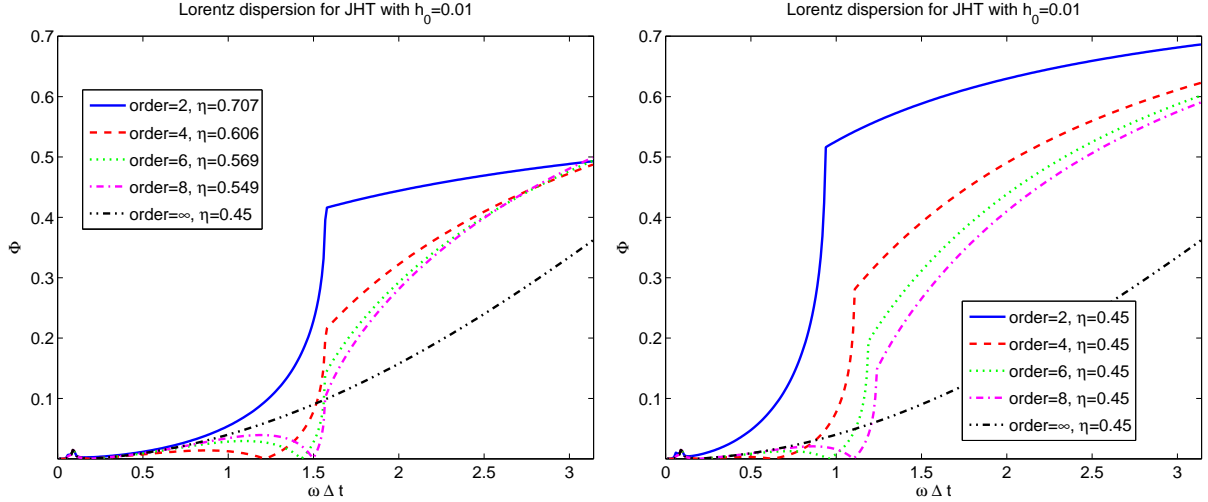


Figure 20: Left and right plots are similar to corresponding plots in Figure 19 except here $h_0 = 0.01$. Note the change in axes from that of Figure 19.

8 Conclusions

We have studied staggered finite difference schemes of arbitrary (even) order in space and second order in time for dispersive materials (Debye and Lorentz) and compared them from

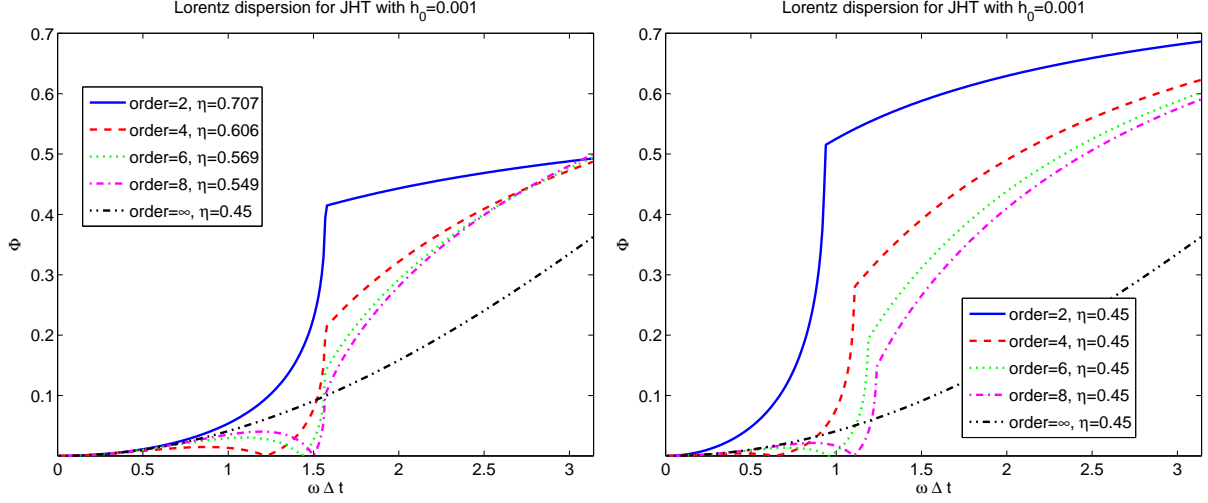


Figure 21: Left and right plots are similar to corresponding plots in Figure 19 except here $h_0 = 0.001$. Note the change in axes from that of Figure 19.

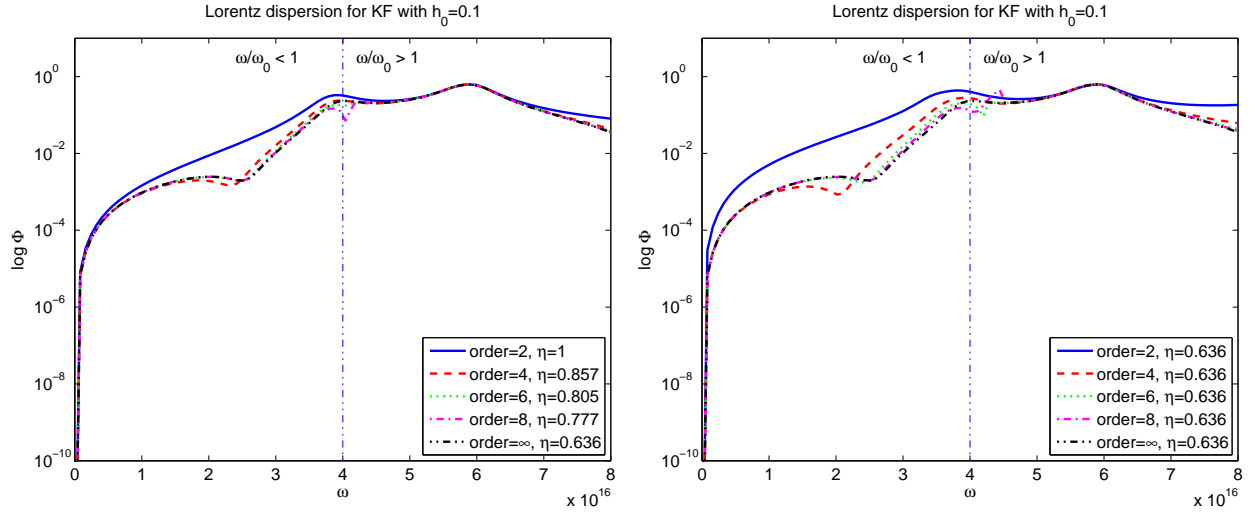


Figure 22: Plot on left is a log plot of the phase error ϕ versus ω using $h_0 = 0.1$ for the KF scheme for the Lorentz model of orders 2, 4, 6, 8 and the limiting (order = ∞) case with η set to the maximum stable value for the order. Vertical line distinguishes region of $\omega/\omega_0 < 1$ from $\omega/\omega_0 > 1$. Plot on right is with η fixed at the maximum stable value for the limiting (order = ∞) case.

the point of view of stability and dispersion. This study was inspired by the work in [31] for second order methods.

For each scheme we have given a necessary and sufficient stability condition which is explicitly dependent on the material parameters and the order of the method. Additionally,

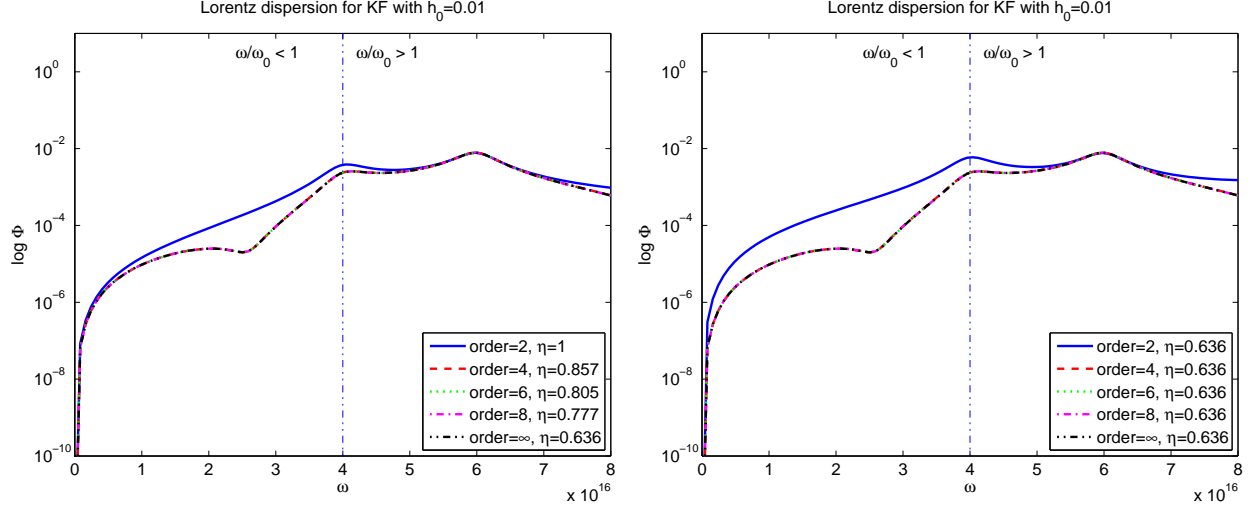


Figure 23: Left and right plot are similar to previous figure except here using $h_0 = 0.01$.

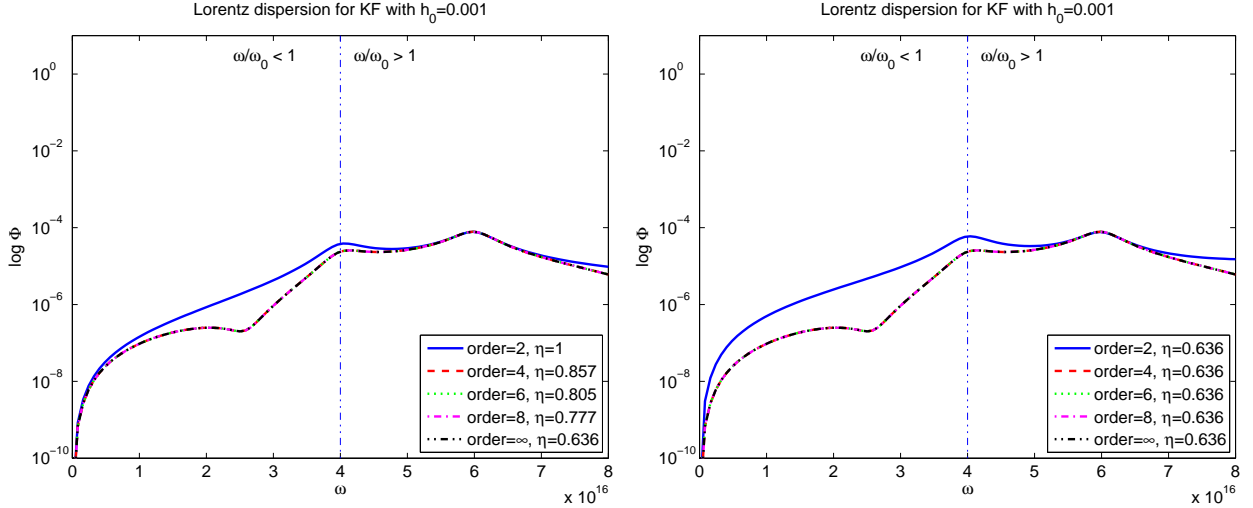


Figure 24: Left and right plot are similar to previous figure except here using $h_0 = 0.001$.

we have found a bound for stability for all orders by computing the limiting (infinite order) case. Further, we have derived a concise representation of the numerical dispersion relation for each scheme of arbitrary order, which allows an efficient method for predicting the numerical characteristics of a simulation of electromagnetic wave propagation in a dispersive material.

From the stability analysis in the paper, we can conclude that the numerical dissipation in the schemes presented here for Debye and Lorentz media are strongly dependent on the temporal resolution (the quantity $h_\tau = \Delta t/\tau$ when τ is the smallest time scale, or for Lorentz media, the quantity $h_0 = \Delta t/T_0$ may be the dominant quantity if $T_0 = 2\pi/\omega_0$ is smaller than τ). We see that h_τ or h_0 has to be sufficiently small in order to accurately model the

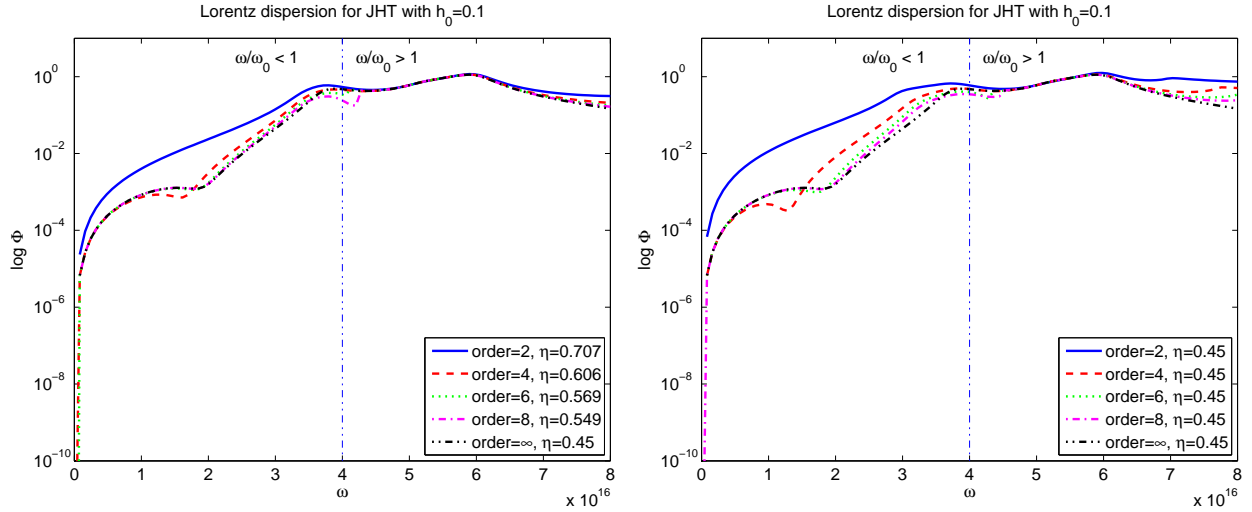


Figure 25: Plot on left is a log plot of the phase error ϕ versus ω using $h_0 = 0.1$ for the JHT scheme for the Lorentz model of orders 2, 4, 6, 8 and the limiting (order = ∞) case with η set to the maximum stable value for the order. Vertical line distinguishes region of $\omega/\omega_0 < 1$ from $\omega/\omega_0 > 1$. Plot on right is with η fixed at the maximum stable value for the limiting (order = ∞) case.

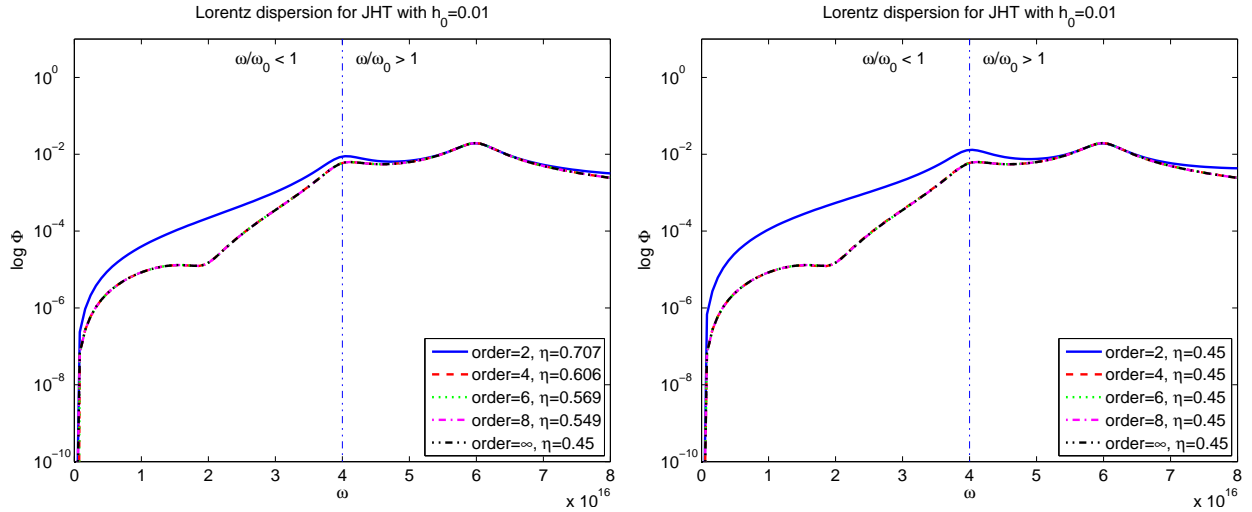


Figure 26: Left and right plot are similar to previous figure except here using $h_0 = 0.01$.

propagation of pulses at large distances inside the dispersive dielectric medium. For higher orders, the stability restriction has the effect of allowing larger wavenumbers to exhibit the same dissipation error as would a smaller wavenumber at a lower order.

From the dispersion analysis we see that the discrete representations of the continuous model parameters are the same regardless of order of the method, only the representation of the wave number changes. Numerical experiments show that the dispersion error for fourth

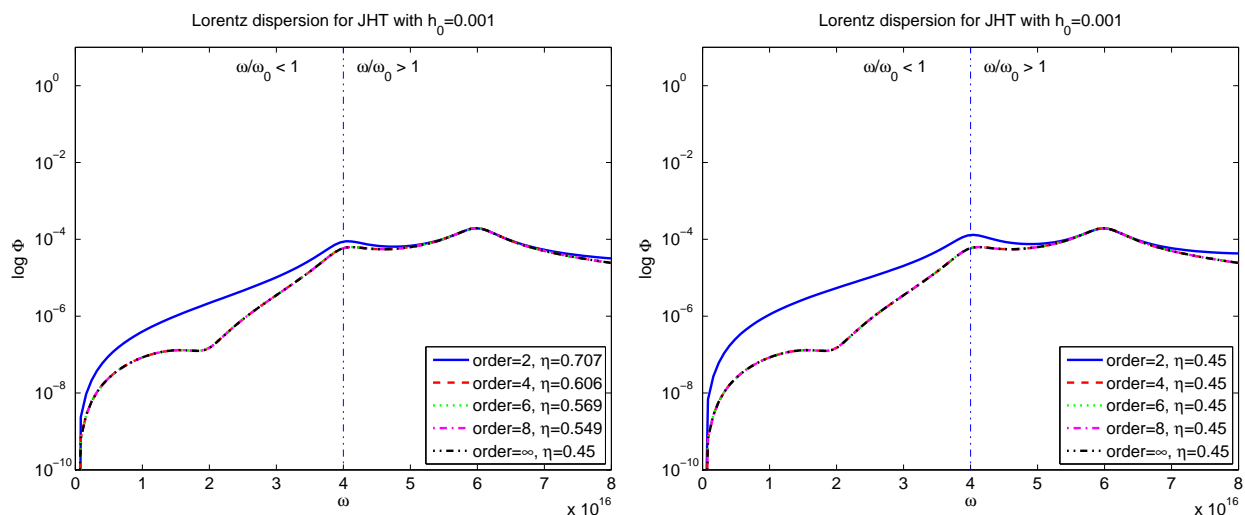


Figure 27: Left and right plot are similar to previous figure except here using $h_0 = 0.001$.

order methods is slightly less than that of second order methods, but no significant gain is achieved by increasing to higher order.

Other higher order simulation methods for dispersive materials may also be analyzed using the approaches described in the current work, including those for the Drude polarization model, the stable-JHT scheme described in [30], those corresponding to collisionless cold plasma [45], and others which are mentioned in [10]. Additionally, any number of multiple poles may be considered in a straight-forward manner, see for example, the fourth and sixth order methods for multi-pole Debye and Lorentz in [35]. The specific stability results from [10] for two and three dimensions, may be extended as well in a similar fashion to the analysis presented here by using a representation of the numerical schemes in a manner as described in [14] for the wave equation.

Acknowledgments

The first author is supported by grant number DMS-0811223 from the NSF Computational Mathematics program.

References

- [1] R. A. Albanese, R. L. Medina, and J. W. Penn. Mathematics, medicine and microwaves. *Inverse Problems*, 10:995–1007, 1994.
- [2] R. A. Albanese, J. W. Penn, and R. L. Medina. Short-rise-time microwave pulse propagation through dispersive biological media. *J. Opt. Soc. Amer. A*, 6:1441–1446, 1989.
- [3] J. C. Anderson. *Dielectrics*. Chapman and Hall, London, 1967.

- [4] L. Anne, P. Joly, and Q. H. Tran. Construction and analysis of higher order finite difference schemes for the 1D wave equation. *Comput. Geosci.*, 4(3):207–249, 2000.
- [5] H. T. Banks, V. A. Bokil, and N. L. Gibson. Analysis of stability and dispersion in a finite element method for Debye and Lorentz dispersive media. *Numer. Methods Partial Differential Equations*, 25(4), 2009.
- [6] H. T. Banks, M. W. Buksas, and T. Lin. *Electromagnetic Material Interrogation Using Conductive Interfaces and Acoustic Wavefronts*, volume FR21 of *Frontiers in Applied Mathematics*. SIAM, Philadelphia, PA, 2000.
- [7] H. T. Banks and N. L. Gibson. Electromagnetic inverse problems involving distributions of dielectric mechanisms and parameters, 2005.
- [8] H. T. Banks and N. L. Gibson. Well-posedness in Maxwell systems with distributions of polarization relaxation parameters. *Appl. Math. Lett.*, 18(4):423–430, 2005.
- [9] I. Barba, A. C. L. Cabeceira, M. Panizo, and J. Represa. Modelling dispersive dielectrics in TLM method. *Int. J. Numer. Model.*, 14:15–30, 2001.
- [10] B. Bidégaray-Fesquet. Stability of FD-TD schemes for Maxwell-Debye and Maxwell-Lorentz equations. *SIAM J. Numer. Anal.*, 46(5):2551–2566, 2008.
- [11] J. G. Blaschak and J. Franzen. Precursor propagation in dispersive media from short-rise-time pulses at oblique incidence. *J. Opt. Soc. Amer. A*, 12:1501–1512, 1995.
- [12] L. Brillouin. *Wave propagation and group velocity*. Academic Press New York, 1960.
- [13] G. Cohen and P. Joly. Construction and analysis of fourth-order finite difference schemes for the acoustic wave equation in nonhomogeneous media. *SIAM J. Numer. Anal.*, 33(4):1266–1302, 1996.
- [14] G. C. Cohen. *Higher-order numerical methods for transient wave equations*. Springer Verlag, 2002.
- [15] K. S. Cole and R. H. Cole. Dispersion and absorption in dielectrics i. alternating current characteristics. *J. Chem. Phys.*, 9:341–351, 1941.
- [16] S. A. Cummer. An analysis of new and existing FDTD methods for isotropic cold plasma and a method for improving their accuracy. *IEEE Trans. Antennas and Propagation*, 45(3):392–400, 1997.
- [17] P. J. W. Debye. *Polar molecules*. The Chemical Catalog Company, inc., 1929.
- [18] E. C. Fear, P. M. Meaney, and M. A. Stuchly. Microwaves for breast cancer detection. *IEEE Potentials*, pages 12–18, 2003.
- [19] B. Fornberg. On a Fourier method for the integration of hyperbolic equations. *SIAM J. Numer. Anal.*, pages 509–528, 1975.

- [20] B. Fornberg and M. Ghrist. Spatial finite difference approximations for wave-type equations. *SIAM J. Numer. Anal.*, 37(1):105–130, 1999.
- [21] M. Ghrist. *Finite Difference Methods for Wave Equations*. PhD thesis, Univ. of Colorado, Boulder, CO., 2000.
- [22] J. D. Jackson. *Classical Electromagnetics*. John Wiley and Sons, New York, 1999.
- [23] R. M. Joseph, S. C. Hagness, and A. Taflove. Direct time integration of Maxwell’s equations in linear dispersive media with absorption for scattering and propagation of femtosecond electromagnetic pulses. *Optics Lett.*, 16(18):1412–1414, 1991.
- [24] H. M. Jurgens and D. W. Zingg. Numerical solution of the time-domain Maxwell equations using high-accuracy finite-difference methods. *SIAM J. Sci. Comput.*, 22(5):1675–1696, 2000.
- [25] T. Kashiwa and I. Fukai. A treatment by the FD-TD method of the dispersive characteristics associated with electronic polarization. *Microwave Opt. Technol. Lett.*, 3(6):203–205, 1990.
- [26] T. Kashiwa, N. Yoshida, and I. Fukai. A treatment by the finite-difference time domain method of the dispersive characteristics associated with orientational polarization. *IEEE Trans. IEICE*, 73(8):1326–1328, 1990.
- [27] D. F. Kelley and R. J. Luebbers. Piecewise linear recursive convolution for dispersive media using FDTD. *IEEE Trans. Antennas and Propagation*, 44(6 Part 1):792–797, 1996.
- [28] R. Luebbers, F. P. Hunsberger, K. S. Kunz, R. B. Standler, and M. Schneider. A frequency-dependent finite-difference time-domain formulation for dispersive materials. *IEEE Trans. Electromagnetic Compatibility*, 32(3):222–227, 1990.
- [29] R. J. Luebbers and F. Hunsberger. FDTD for Nth-order dispersive media. *IEEE Trans. Antennas and Propagation*, 40(11):1297–1301, 1992.
- [30] A. Pereda, L. A. Vielva, A. Vegas, and A. Prieto. Analyzing the stability of the FDTD technique by combining the vonNeumann method with the Routh-Hurwitz criterion. *IEEE Trans. Microwave Theory and Techniques*, 49(2):377–381, 2001.
- [31] P. Petropoulos. Stability and phase error analysis of FD-TD in dispersive dielectrics. *IEEE Trans. Antennas and Propagation*, 42(1):62–69, 1994.
- [32] P. G. Petropoulos. The wave hierarchy for propagation in relaxing dielectrics. *Wave Motion*, 21:253–262, 1995.
- [33] K. P. Prokopidis, E. P. Kosmidou, and T. D. Tsiboukis. An fdtd algorithm for wave propagation in dispersive media using higher-order schemes. *J. Electromagn. Waves Applicat.*, 18:1171–1194, 2004.

- [34] K. P. Prokopidis and T. D. Tsiboukis. FDTD algorithm for microstrip antennas with lossy substrates using higher order schemes. *Electromagn.*, 24(5):301–315, 2004.
- [35] K. P. Prokopidis and T. D. Tsiboukis. Higher-order spatial fdtd schemes for em propagation in dispersive media. In *Electromagnetic fields in mechatronics, electrical and electronic engineering: proceedings of ISEF'05*, page 240. Ios Pr Inc, 2006.
- [36] R. Siushansian and LoVetri J. A comparison of numerical techniques for modeling electromagnetic dispersive media. *IEEE Microwave Guided Wave Lett.*, 5:426–428, 1995.
- [37] J. C. Strikwerda. *Finite difference schemes and partial differential equations*. Society for Industrial Mathematics, 2004.
- [38] D. M. Sullivan. A frequency-dependent FDTD method for biological applications. *IEEE Trans. Microwave Theory and Techniques*, 40(3):532–539, 1992.
- [39] D. M. Sullivan. Z-transform theory and the FDTD method. *IEEE Trans. Antennas and Propagation*, 44(1):28–34, 1996.
- [40] A. Taflove and S. C. Hagness. *Computational Electrodynamics: The Finite-Difference Time-Domain method*. Artech House, Norwood, MA, 3rd edition, 2005.
- [41] L. N. Trefethen. Group velocity in finite difference schemes. *SIAM Rev.*, 24:113–136, 1982.
- [42] Z. Xie, C. Chan, and B. Zhang. An explicit fourth-order staggered finite-difference time domain method for Maxwell's equations. *J. Comp. Appl. Math.*, 147:75–98, 2002.
- [43] A. Yefet and P. Petropoulos. A Staggered Fourth-Order Accurate Explicit Finite Difference Scheme for the Time-Domain Maxwell's Equations. *J. Comput. Phys.*, 168:286–315, 2001.
- [44] A. Yefet and P. G. Petropoulos. A fourth-order FD-TD scheme for electromagnetics. In *Mathematical and numerical aspects of wave propagation (Santiago de Compostela, 2000)*, pages 883–887. SIAM, Philadelphia, PA, 2000.
- [45] J. Young. A higher order fdtd method for em propagation in a collisionless cold plasma. *IEEE Trans. Antennas and Propagat.*, 44(9):1283–1289, 1996.
- [46] J. Young, D. Gaitonde, and J. Shang. Toward the construction of a fourth-order difference scheme for transient em wave simulation: Staggered grid approach. *IEEE Trans. Antennas and Propagat.*, 45(11):1573–1580, 1997.
- [47] J. L. Young, A. Kittichartphayak, Y. M. Kwok, and D. Sullivan. On the Dispersion errors related to (FD)²TD type schemes. *IEEE Trans. Microwave Theory and Techniques*, 43(8):1902–1910, 1995.
- [48] J. L. Young and R. O. Nelson. A summary and systematic analysis of FDTD algorithms for linearly dispersive media. *IEEE Antennas and Propagation Magazine*, 43:61–77, 2001.